

VAPORIZATION INTERFACE PROPAGATION
THROUGH A ONE-DIMENSIONAL
POROUS SLAB

By

LAWRENCE BARRY SAMARTIN

Bachelor of Arts

Newark State College

Union, New Jersey

1963

Submitted to the Faculty of the Graduate College
of the Oklahoma State University
in partial fulfillment of the requirements
for the Degree of
MASTER OF SCIENCE
May, 1973

12/14/73
12/14/73
12/14/73

12/14/73

12/14/73

Thesis
1973
518"V
Cop. 2.

12/14/73

12/14/73

12/14/73

12/14/73

12/14/73
12/14/73
12/14/73
12/14/73

JUN 1 1973

VAPORIZATION INTERFACE PROPAGATION
THROUGH A ONE-DIMENSIONAL
POROUS SLAB

Thesis Approved:

W. B. Brooks

Thesis Adviser

M. L. Liederman, Jr.

D. Hurham

Dean of the Graduate College

ACKNOWLEDGMENTS

I would like to express my appreciation for the guidance and assistance given me by my adviser, Dr. William Brooks. I would also like to thank Dr. William Tiederman and Dr. Ronald Panton for their interest and encouragement; Mrs. Lynn Danvers for her patience, advice and excellent typing; and my wife Lucille for her understanding, encouragement and financial assistance. The research for this study was supported by the Air Force Armament Laboratory for which I am extremely grateful.

TABLE OF CONTENTS

Chapter	Page
I. INTRODUCTION	1
The Complete Problem	2
Division Into Cases of Study	2
Pyrolysis and Ignition of a Porous Solid	3
The Change of Phase Phenomena	6
Scope of the Present Study	8
II. PROBLEM ANALYSIS	10
Physical Model	10
Energy Equation	13
Initial and Boundary Conditions	21
Non-Dimensionalization	24
III. MATHEMATICAL SOLUTION	27
Background	27
Application of the Integral Method	29
Initial Conditions	37
Computer Technique	38
Method of Numerical Integration	38
IV. COMPUTATIONAL RESULTS	42
Inert Solution	42
Constant and Parameter Values	42
Temperature Relations	44
Interface Velocity	47
Pyrolysis Retardation	50
V. SUMMARY AND CONCLUSIONS	54
Summary	54
Conclusions	55
BIBLIOGRAPHY	57
APPENDICES	
A. EFFECTS OF VAPOR EFFLUX	60

APPENDICES	Page
B. NON-DIMENSIONALIZATION OF EQUATIONS AND BOUNDARY CONDITIONS	64
C. INTEGRATION OF EQUATION (3.1)	70
D. INTEGRATION OF EQUATION (3.3)	72
E. DERIVATION OF EQUATIONS (3.10) AND (3.11)	74
F. DERIVATION OF EQUATION (3.13)	77
G. INTEGRATION OF EQUATION (3.14)	79
H. EVALUATION OF PARAMETERS \bar{A} AND \bar{K}	81
I. COMPUTER PROGRAM LISTING	83

LIST OF TABLES

Table	Page
I. Non-Dimensional Variables	25
II. Non-Dimensional Parameters	25
III. Computer Program Cycle	39
IV. Dimensional Constants and Parameters	46

LIST OF FIGURES

Figure	Page
1. Pyrolysis Reactions in the Slab	5
2. Physical Model	11
3. Volume Element of the Saturated Slab	14
4. Vaporization Represented as a Chemical Reaction	18
5. Vaporization Represented as a Surface Phenomena	18
6. Comparison of Approximate Solution of Inert Slab With Exact Solution	43
7. Selected Temperature Profiles With Respect to Time	45
8. Temperature Profile of Slab at Selected Time Intervals	48
9. Interface Velocity With Respect to Distance	49
10. Effect of Heat of Reaction: Temperature History of Front and Back Surfaces - Constant Heat Flux, One Exothermic Reaction	51

NOMENCLATURE

A	area
A_i	time dependent, Fourier cosine series coefficient i of the temperature approximation
a_i	rate constant for reaction i
C	mean specific heat
C_p	constant pressure specific heat
c	constant
E_i	activation energy for reaction i
G	heat flux parameter considered unity in this study (see Appendix I)
g	standard gravitational acceleration
g_c	gravitational dimension constant
h	enthalpy
h_{fg}	enthalpy of vaporization
K	thermal conductivity
L	slab thickness, between heated and insulated surfaces
l	vaporization interface distance from insulated surface
N	one less than the number of coefficients used in the temperature approximation
P	pressure
Q	weighting function in x
q	heat flux

R universal gas constant
 T temperature
 t time
 u internal energy
 V volume
 v velocity
 \hat{v} specific volume
 x slab distance from insulated surface
 y_i integrated value of derivative x_i

Greek Letters

α thermal diffusivity
 μ integrating factor
 ρ density
 τ_{xx} viscous stress on the plane normal to the x axis in the x direction

Subscripts

A actual
 b back (insulated) surface
 D dry region
 i index $i = 0, 1, 2, \dots, N$
 l liquid
 m index $m = 0, 1, 2, \dots, N$
 n index $n = 0, 1, 2, \dots, N$
 o front (heated) surface
 R reference
 s solid
 v vapor

W wet region

z non-dimensionalization variable

Superscripts

' differentiation with respect to x

— (bar) non-dimensional variable

- (minus) dry side of the vaporization interface

+ wet side of the vaporization interface

Note: A superscript bar is used to denote non-dimensional representation of the symbols as defined in Table I.

CHAPTER I

INTRODUCTION

For thousands of years man has known that wet logs do not burn as well as dry ones. He has also learned that liquids can be used effectively to douse certain unwanted fires. Man has thus studied the burning process for two opposing reasons. On one hand he has sought to improve this process as a tool for constructive uses and on the other hand he has sought to find ways to disrupt this process to protect himself from uncontrolled fires.

Since porous substances (such as wood, paper, fiber board, etc.) contain varying amounts of liquid when exposed to the natural environment, the burning of these materials is affected by the presence of this liquid. Yet, this extra-cellulosic liquid has been ignored in analytic studies of the thermal decomposition of porous materials. Considered as a fire retardant, the vaporization of a liquid possessing a high boiling point, a high latent heat of vaporization, and a relatively low thermal conductivity will reduce the overall temperature of the material in which it was saturated. Thereby the thermal decomposition will be retarded and the time to ignition of the substance will be increased.

It is advantageous, then, to study the effects caused by applying a heat flux to various substances initially saturated with some particular liquid. The calculation of the time required for the system to reach the temperature of vaporization of the liquid, the rate at which the

liquid-vapor interface propagates through the system, the temperature throughout the system, and time to ignition of the substance would aid considerably in the study of the burning process and fire retardation.

The Complete Problem

The time dependent temperature distribution within a saturated porous material (i.e. wood saturated with water) exposed to a heat flux may be calculated somewhat easily provided that the temperature distribution is not sufficiently high to cause vaporization of the liquid present or pyrolysis (thermal decomposition) of the material. If this condition on the temperature is not satisfied the problem of determining the temperature distribution becomes appreciably complicated and must include the endothermic process of vaporization and the endothermic or exothermic reactions of pyrolysis. A complete examination of the heating of a saturated porous material therefore would include determining the temperature distribution within the saturated material, the position and nature of the liquid-vapor interface as vaporization of the liquid progresses, the temperature distribution within the porous material after vaporization of the liquid initially present, and the pyrolysis and subsequent ignition of the material.

Division Into Cases of Study

Since wood is still one of the widest used porous materials and the thermal decomposition of wood closely follows that of cellulose, a reasonable choice of constituents for this problem is cellulose and water. The thermal decomposition of cellulose has been shown to be minimal below 300° C (2,21). At standard pressure the vaporization of

water occurs at 100°C. Therefore, with the proper choice of material and liquid, decomposition of the porous material can be neglected below the temperature of vaporization of the liquid. The complete examination of the heating of a saturated porous material can then be divided into two cases, or areas, of investigation. The first case is the study of the temperature distribution within the porous material from the initial application of the heat flux up to and including the vaporization of the liquid and the propagation of the liquid-vapor interface through the material. The second case is comprised of the pyrolysis and ignition of the dried porous material remaining after vaporization of the liquid. The following sections briefly describe previous investigations of each case.

Pyrolysis and Ignition of a Porous Solid

The pyrolysis of wood has been studied both analytically and experimentally by Bamford, Crank and Malan (3). An infinite slab of wood was considered, symmetrically heated by a flame on each face. One exothermic reaction was included in the one-dimensional energy equation of the form

$$-q \frac{\partial \omega(x,t)}{\partial t}$$

where q is the heat liberated at constant pressure per gram of volatile products evolved, $\omega(x,t)$ is the weight of these products per cubic centimeter of wood. The rate of change of density (ω) with respect to time was represented by the Arrhenius expression

$$\frac{\partial \omega(x,t)}{\partial t} = k \omega \exp(-E/RT)$$

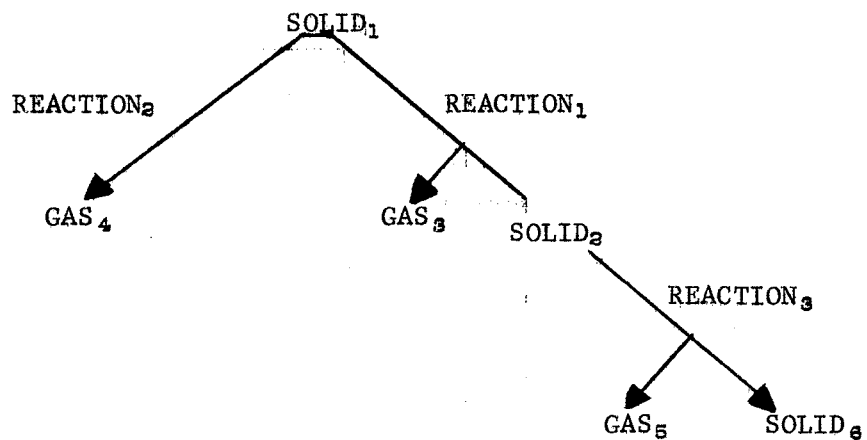
in which k is a frequency of molecular collision constant and E is the

activation energy of the reaction (assumed constant) (22). Although samples used in the experimental study contained moisture up to 11%, no additional endothermic reaction was included in the analytic study to represent the vaporization of extra-cellulosic moisture. The heat flux applied to the slab was considered a function of the surface temperature given by Fourier's Heat Conduction Law.

The analysis of a dry porous solid undergoing pyrolysis was substantially extended by Rittmann (21). Three chemical reactions were considered, two occurring simultaneously (competitive in nature) and two occurring consecutively (Figure 1). In the case of cellulose the first reaction is endothermic causing the pure cellulose to lose water and form a dehydrocellulose. This reaction was assumed to occur after vaporization of any extra-cellulosic moisture. Rittmann examined separately a time dependent, radiative heat flux and a constant, convective heat flux. Also the effect of a density dependent thermal conductivity was investigated.

One criteria for ignition of porous material (cellulose), which has been experimentally substantiated, is a temperature of approximately 600°C on the exposed surface of the slab. Martin (14) observed spontaneous-flaming ignition when the exposed surface of alpha-cellulose sheets reached a constant temperature in the range of 600° - 650° C. Alvares (1) employed optical temperature measurement techniques and obtained consistent temperatures of approximately 600° C on the exposed surface of alpha-cellulose at the onset of ignition regardless of the magnitude of the radiant heat flux.

Weatherford and Sheppard (25) examined the overall effects of various ignition criteria and the surface temperature histories of



Reactions 1 and 2 are competitive.

Reactions 1 and 3 are consecutive.

For Cellulose:

Solid₁ = original cellulose

Solid₂ = "dehydrocellulose"

Gas₃ = water vapor

Gas₄ = "tar" (levoglucosan)

Gas₅ = CO, CO₂, H₂O, etc.

Solid₆ = char

Figure 1. Pyrolysis Reactions in the Slab, Rittman (21)

finite-thickness slabs as opposed to the infinitely thick slab. The authors present a thermal feedback theory in which initial thermal energy received instantaneously at the surface of symmetry is visualized as moving back through the slab to the heated surface by a random self-diffusion process. This criteria is correlated with sustained ignitions which are dependent on the thickness of the slab. Alvares and Martin (2), conducting pyrolysis experiments on cellulose in "artificial airs" composed of different combinations of nitrogen, helium and carbon dioxide, have ruled out the concept that spontaneous ignition is triggered by the appearance of reactive species in the pyrolysis. Their hypothesis is one of thermal autoignition dependent on total pressure, oxidant concentration and inert diluent used.

The Change of Phase Phenomena

The change of phase phenomena is manifest in many physical processes involving heat transfer. The solidification of castings, freezing and thawing of soils and food stuffs, burning of liquid fuels, fusing of various metals, and the ablation process are a few examples. Literature pertaining to the analytic study of vaporization with consideration given to the location of the liquid-vapor interface is not readily available. Much work, however, has been done on the freezing and melting problem involving the location of the solid-liquid interface.

Muehlbauer and Sunderland (15) offer a comprehensive survey of publications dealing with the melting and freezing of infinite and semi-infinite slabs from Stephen's initial discussion of the problem

up to Moon and Keeler who use quantum mechanics to explain the electronics and phonon heat conduction between regions in contact.

Murray and Landis (16) review various methods of solution for the melting or freezing problem and propose two schemes for solution by finite difference approximations. One scheme is to divide the solid region into r equally sized space increments of

$$\Delta x_s = \frac{\epsilon}{r}$$

(where ϵ is the position of the interface) which increases as the freezing front progresses and a liquid region divided into $N-r$ equally spaced intervals

$$\Delta x_L = \frac{E - \epsilon}{N - r}$$

(E being the length of the slab) which shrink with time. The second scheme is to have fixed "lump" sizes where the interface is in the q^{th} lump at some intermediate time. Two temperatures are calculated by interpolation from temperatures in the solid and liquid regions, respectively, using the fusion temperature and the fusion front location. The authors state that the variable space network is preferable for evaluation of the fusion front travel while the fixed space network is more convenient for temperature representation.

Both of the above methods produce two singularities within the finite difference equations when $\epsilon = 0$ and $E = \epsilon$. Therefore the problem must be started with an assumed initial value of ϵ and an assumed temperature distribution in the solid region. This procedure can lead to instability of the solution caused by very small numerical values or by a step input condition as a result of improper choice of initial temperatures. Lazaridis (12) presents a method to extend the finite

difference technique to multidimensional configurations. Longwell (13) developed a unique extension to the Schmidt graphical method. In solving the freezing problem the time for the interface to move a distance Δx is calculated by moving the interface a distance Δx , and then performing Schmidt constructions in each phase. The Newmann problem is solved by this method and compared to the exact solution with good agreement.

Goodman and Shea (10) assumed the applied heat flux at one surface of a semi-infinite slab was not immediately felt throughout the slab. A time dependent region extending from the surface into the slab was defined as the thermal-layer thickness. The heat conduction equation was then reduced by integrating over this defined region. This method of integral solution will only satisfy the original heat conduction equation on the average and is dependent on the time required for the thermal-layer to develop.

Scope of the Present Study

The object of this study is to develop an analytic model of the vaporization interface propagation and the temperature distribution within a semi-infinite, porous slab prior to pyrolysis. A constant, radiative heat flux is applied to the slab which is initially saturated with a liquid.

The semi-infinite slab is divided into two regions by the vaporization interface. Three energy balance equations are developed by application of the first law of thermodynamics to a differential volume in each region and at the interface then taking the limit as the thickness approaches zero. The integral method of reducing partial

differential equations is employed enabling the combination of the three energy equations into one.

By choosing $\cos n\pi\bar{x}$ for the weighting function and the Fourier cosine series to approximate the temperature, a system of ordinary first order differential equations is developed. This system of equations yields valid temperatures for any location within the slab. Hamming's modified predictor-corrector method of numerical integration is then used to solve this system of equations for the temperature coefficients and the interface distance.

As explained in Chapter II, the kinetic and potential energies of the system are assumed negligible. The densities and thermodynamic properties are assumed to be constant with the density and thermodynamic properties for the two component region calculated on a percent unit volume basis.

The analysis is developed for an idealized liquid and solid. The assumption is made that the thermodynamic properties of the liquid and solid are equal in each region as discussed in Chapter II. Complexities of solution and enhancements which might be incorporated in future investigations are mentioned. The resulting temperature profiles and the interface velocity are physically realistic. The coupling of this study with the analysis of chemical reactions can then be employed to solve the complete pyrolysis problem.

CHAPTER II

PROBLEM ANALYSIS

Physical Model

To model the heating of a saturated porous material without simplification is an extremely difficult task. The following factors might be considered in the analysis:

1. Environment of the model
2. Nature of the applied heat flux
3. Size and shape of the material
4. Variations in the thermodynamic properties
5. Representation of the pyrolysis reactions
6. Criteria to determine ignition
7. Representation of the vaporization process.

The model presented here is assumed to be of a semi-infinite, homogeneous (with respect to density and thermodynamic properties), porous slab of thickness L , initially saturated with a homogeneous liquid in thermodynamic equilibrium at a reference temperature (T_R). The front surface ($x = L$) is exposed to a constant, radiative heat flux (q_0) with the back surface ($x = 0$) insulated against heat transfer (Figure 2). This is similar to one-half a slab of thickness $2L$ symmetrically heated. Heat is transferred into the saturated slab from the surface by conduction. None of the radiant energy striking the slab is assumed to penetrate below the surface.

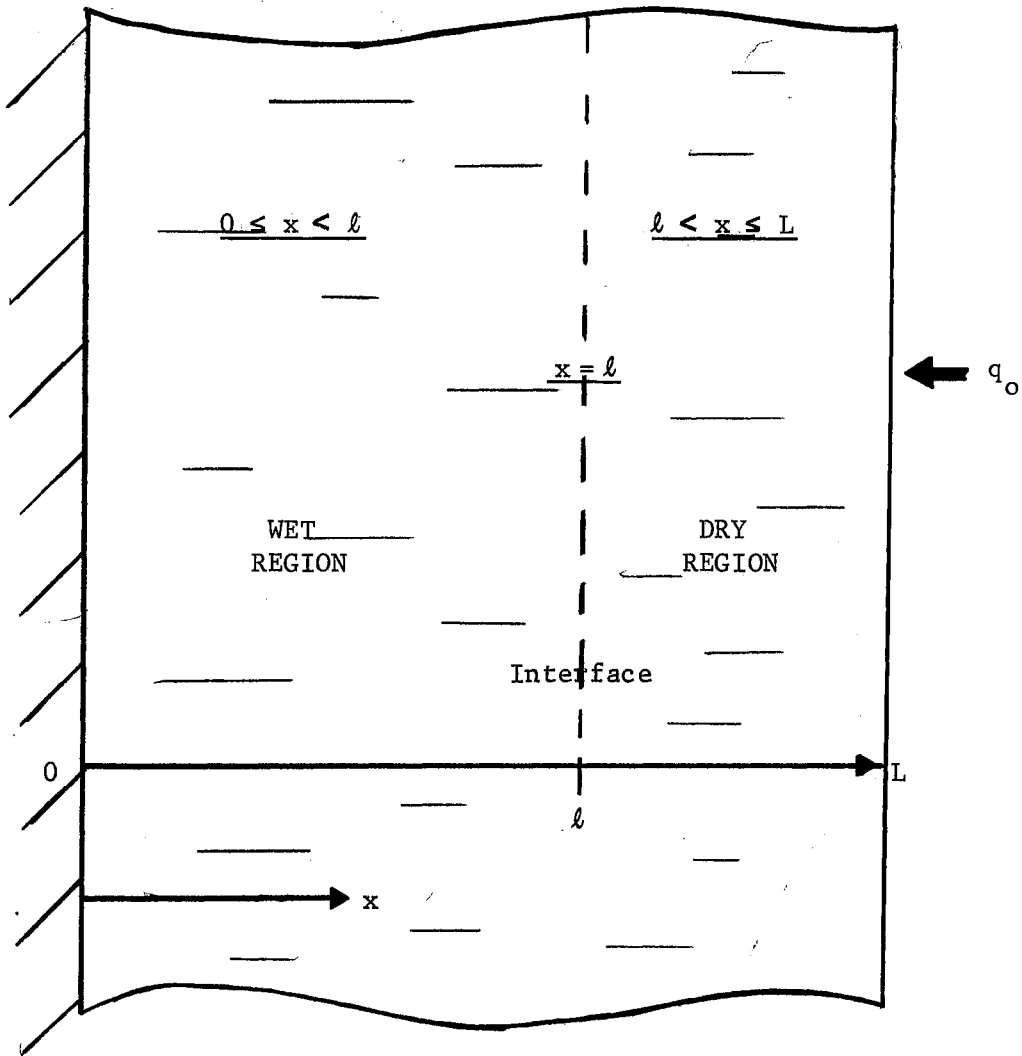


Figure 2. Physical Model

No ignition or chemical reaction of the porous slab is considered. Vaporization of the liquid is considered when the front surface has reached the temperature of vaporization (T_v) of the liquid. At this point in time, vaporization of the liquid is assumed to commence. Heat transfer from and the thermal capacitance of the vapor thus produced is neglected as it flows out through the pores of the slab.¹

As the heat flux is continually applied the time dependent liquid-vapor interface proceeds into the slab in the $-x$ direction, thereby dividing the slab into regions, a wetted region preceding the interface and a dry region behind. The wetted region consequently shrinks with increasing time as the dry region expands. As stated previously the wetted region is considered non-reactant since its temperature will remain well below that which is necessary to cause significant chemical reaction provided the proper choice of solid and liquid is made.

The pyrolysis of the dry region (second case investigation) can be modeled after the extensive work of Rittmann (21). If the overall effects of pyrolysis leading to the ignition of the solid is of main interest a single endothermic or exothermic reaction will suffice in representing a lumped form of the pyrolysis as done by Bamford, Crank, and Malan (3).

Experimental and analytic research indicates that the ignition of the porous solid can be approximated as the point in time at which the front surface of the semi-infinite slab exceeds 600°C . Thus the effects, caused by the initial presence of a liquid, on the ignition

¹For a discussion of this assumption see Appendix A.

time of a porous solid can be directly related to the surface temperature. This investigation is left to future studies.

Energy Equation

The energy equation for a semi-infinite saturated slab is developed by writing an energy balance over a volume element $\Delta x \Delta y \Delta z$ in the x direction then taking the limit as these dimensions approach zero. Considering only the fluid, the following equation evolves from Figure 3.

$$\begin{aligned}
 \frac{\partial}{\partial t} \rho_l \left[u_l + \frac{1}{2} v_l^2 + \frac{g}{g_c} z \right] &= - \frac{\partial}{\partial x} \left(\rho_l v_l u_l \right) - \frac{\partial}{\partial x} \left(v_l \rho_l \frac{v_l^2}{2} \right) \\
 \text{I} & \qquad \qquad \qquad \text{II} \qquad \qquad \qquad \text{III} \\
 & - \frac{\partial}{\partial x} q_l + \frac{\partial}{\partial x} \left(\rho_l \frac{g}{g_c} v_l z \right) \\
 & \qquad \qquad \qquad \text{IV} \qquad \qquad \qquad \text{V} \\
 & - \frac{\partial}{\partial x} \left(\rho_l v_l \right) - \frac{\partial}{\partial x} \left(\tau_{xx} v_l \right) \qquad \qquad \qquad (2.1) \\
 & \qquad \qquad \qquad \text{VI} \qquad \qquad \qquad \text{VII}
 \end{aligned}$$

where

- Term I = Rate of change of energy per unit volume.
- Term II = Net rate of internal energy input per unit volume by convection.
- Term III = Net rate of kinetic energy input per unit volume by convection.
- Term IV = Net rate of energy input per unit volume by conduction.
- Term V = Rate of work done on the fluid per unit volume by gravitational forces.

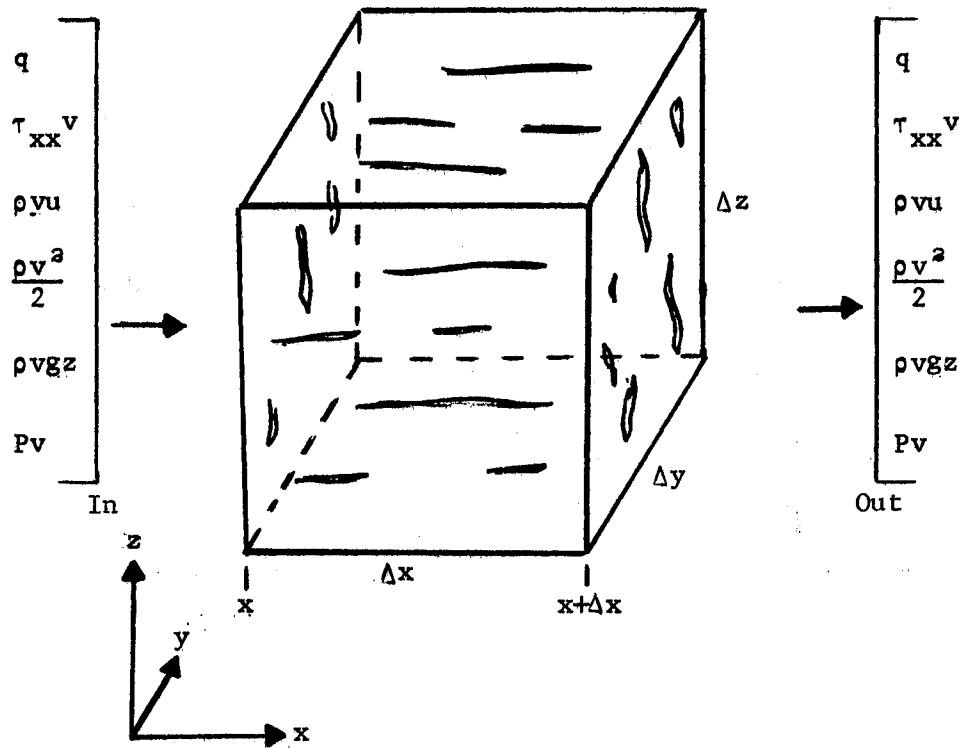


Figure 3. Volume Element of the Saturated Slab

Letting the internal energy be a function of temperature only

$$u = u(T)$$

Then

$$du = \left(\frac{\partial u}{\partial T} \right) dT = c dT$$

Differentiation of term I yields

$$\begin{aligned} \rho_T c_T \frac{\partial T}{\partial t} + u_T \frac{\partial \rho_T}{\partial t} + \frac{\partial}{\partial t} \rho_l \frac{1}{2} v_l^2 = - \frac{\partial}{\partial x} q_T - \frac{\partial}{\partial x} \rho_l v_l \left[u_l + \frac{1}{\rho_l} P_l \right] \\ - \frac{\partial}{\partial x} \rho_l v_l \frac{v_l^2}{2} \end{aligned} \quad (2.5)$$

I
II
III
IV
V

VI

Term II in equation (2.5) the absorption or generation of thermal energy, is frequently represented by one or several chemical reactions of the form;

$$q_i \frac{\partial \rho_i}{\partial t} = q_i \rho_i a_i \exp \frac{-E_i}{RT}$$

where q_i is the latent heat liberated or absorbed, a_i is a maximum rate constant, E_i is the energy of activation required, and R is the universal gas constant. Many authors have shown this expression to closely approximate chemical reactions within the same order of magnitude as the energy change and conduction terms (I and III) of the energy equation (2.5).

If such a function is used to approximate the vaporization process the vaporization is then distributed throughout the slab (i.e. for any given temperature, some vaporization is attained). A plot of

$$q_v \frac{\partial \rho_l}{\partial t}$$

versus temperature (T_v) shows that the vaporization is distributed mainly between $T_v - \Delta T$ and $T_v + \Delta T$ (Figure 4).²

When vaporization is considered a surface occurrence, the density of the liquid becomes zero at some infinitely small distance Δx from the surface. Vaporization of a liquid also occurs at a constant temperature thus the vaporization process appears as plotted in Figure 5. To accomplish this the reaction rate of the function must be very high.

$$\lim_{\rho_l \rightarrow 0} \frac{\partial \rho_l}{\partial t} \rightarrow \infty$$

This would require the time associated with the approximation of

$$q_v \frac{\partial \rho_l}{\partial t}$$

to be very fast as compared to the time associated with the other reactions and terms in the energy equation.

In lieu of the above, the semi-infinite slab is modeled by dividing it into two regions separated by the liquid-vapor interface (Figure 2). The energy equation (2.5) is thus the summation of three energy balances, one applying to each region and one at the interface. The thermodynamic properties of each region considered constant within the range of temperatures to be encountered yields the following energy equations: For the wetted region ($0 \leq x < l$) the fluid is considered stationary with no generation or absorption of thermal energy. Therefore, energy equation (2.5) reduces to

$$\rho_w c_w \frac{\partial T}{\partial t} = - \frac{\partial}{\partial x} q_w$$

² In this instance q_v represents the latent heat of vaporization, ρ_l the density of the liquid, and T_v the temperature of vaporization.

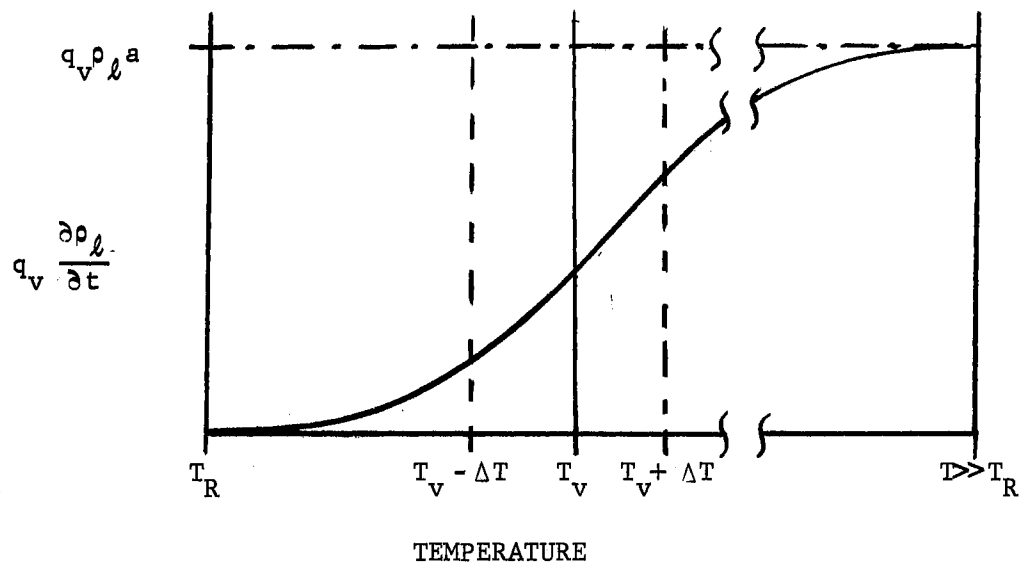


Figure 4. Vaporization Represented as a Chemical Reaction

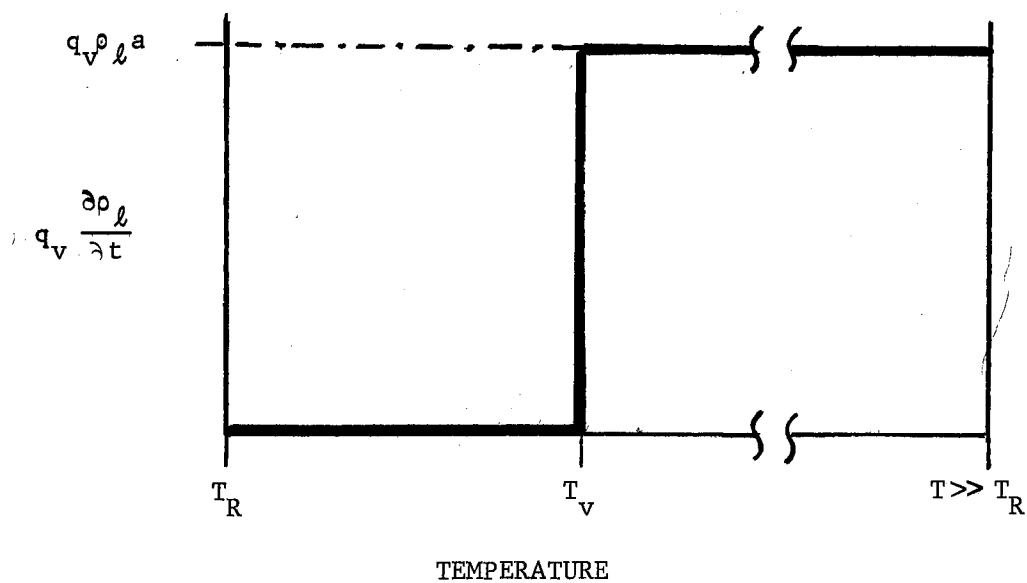


Figure 5. Vaporization Represented as a Surface Phenomena

Applying Fourier's Heat Conduction Law with the temperature gradient in the negative x direction yields

$$\rho_W C_W \frac{\partial T}{\partial t} = K_W \frac{\partial^2 T}{\partial x^2} \quad (2.6)$$

The internal energy, being an extensive thermodynamic property, is additive for a composite system.

$$u_W = u_s + u_l$$

differentiating

$$C_W dT = C_s dT + C_l dT$$

or

$$\rho_W V_W C_W = \rho_s V_s C_s + \rho_l V_l C_l$$

$$\rho_W C_W = \rho_s \frac{V_s}{V_W} C_s + \rho_l \frac{V_l}{V_W} C_l$$

For the dry region ($l < x \leq L$) including the generation or absorption of thermal energy from equation (2.5)

$$\begin{aligned} \rho_D C_D \frac{\partial T}{\partial t} + u_D \frac{\partial \rho_D}{\partial t} + \frac{\partial}{\partial t} \rho_v \frac{1}{2} v_v^2 &= K_D \frac{\partial^2 T}{\partial x^2} + \frac{\partial}{\partial x} \rho_v v_v \left[u_v + \frac{1}{\rho_v} P_v \right] \\ \text{I} \quad \quad \quad \text{II} \quad \quad \quad \text{III} \quad \quad \quad \text{IV} \quad \quad \quad \text{V} \\ &+ \frac{\partial}{\partial x} \rho_v v_v \frac{v_v^2}{2} \quad (2.7) \\ &\quad \quad \quad \text{VI} \end{aligned}$$

Terms III and VI are kinetic energy terms. If the velocity of the vapor escaping is assumed small in magnitude these kinetic energy terms can be neglected. Term V can be rearranged as follows; since

$$\frac{1}{\rho_v} = \hat{v}_v \quad (\text{specific volume})$$

$$\frac{\partial}{\partial x} \rho_v v_v \left[u_v + \frac{1}{\rho_v} P_v \right] = \frac{\partial}{\partial x} \rho_v v_v \left[u_v + P_v \hat{v}_v \right]$$

from the definition of enthalpy

$$h = u + P\hat{v}$$

and

$$\frac{\partial}{\partial x} \rho_v v_v \left[u_v + P_v \hat{v}_v \right] = \frac{\partial}{\partial x} \rho_v v_v (h_v)$$

This term is then the thermal energy convected by the vapor as it flows through the dry region. The magnitude of which is discussed in Appendix A. This convection term is assumed of minimum consequence in this study. The heat capacity of the vapor is also assumed to be negligible in the final energy equation of the dry region. Thus the heat capacity of the dry region is assumed equal to that of the solid alone. Therefore, equation (2.7) is reduced to

$$\rho_D C_D \frac{\partial T}{\partial t} + u_D \frac{\partial \rho_D}{\partial t} = K_D \frac{\partial^2 T}{\partial x^2} \quad (2.8)$$

At the liquid-vapor interface ($x = l$) the volume element (Figure 3) is considered to move in the negative x direction with a velocity dl/dt . The mass flow of fluid entering this moving volume equals the mass flow of vapor leaving, thus satisfying mass conservation. The time rate of change of kinetic energy is assumed zero. Within this elemental volume the temperature is constant and the densities of the liquid and vapor are also assumed constant. Thus equation (2.5) reduces to

$$\frac{\partial}{\partial x} \rho_l \frac{dl}{dt} \left[u_l + \hat{v}_l P_l \right] = \frac{\partial}{\partial x} q$$

Integrating with respect to x yields

$$\rho_l h_{fg} \frac{dl}{dt} \Big|_{l^+}^{l^-} = q \Big|_{l^+}^{l^-}$$

or

$$\rho_l h_{fg} \frac{dl}{dt} \Big|_{l^+}^{l^-} = K_D \frac{\partial T}{\partial x} \Big|_{l^-} - K_W \frac{\partial T}{\partial x} \Big|_{l^+}$$

with the limit as the length Δl approaches zero

$$\rho_l h_{fg} \frac{dl}{dt} = K_D \frac{\partial T}{\partial x} \Big|_{l^-} - K_W \frac{\partial T}{\partial x} \Big|_{l^+} \quad (2.9)$$

I II III

Term I = Rate of change of the internal energy of the liquid per unit volume plus the rate of work done on the fluid per unit volume by pressure forces.

Term II = Energy leaving the interface by conduction per unit volume.

Term III = Energy entering the interface by conduction per unit volume.

Initial and Boundary Conditions

Initially the saturated slab is at a constant temperature (T_R) throughout with an insulated boundary (back surface) at $x = 0$ and an exposed boundary (front surface) at $x = L$. The initial conditions at $t = 0$ are

$$T(x,0) = T_R \quad (2.10)$$

$$\rho_D C_D = \rho_S C_S \quad (2.11)$$

$$\rho_W C_W = \rho_S \frac{V_S}{V_W} C_S + \rho_l \frac{V_l}{V_W} C_l \quad (2.12)$$

$$\rho_i(x,0) = 0 \quad (2.13)$$

where $\rho_1(x,t)$ is the density of the substance remaining or the products produced after some amount of chemical reaction (1) has taken place when pyrolysis is considered (second case of study).

With the introduction of a heat flux (q_0) at the front surface the process is initiated. The entire slab is represented as the wetted region until the time (t_v) at which the front surface reaches the temperature of vaporization of the liquid (T_v). The boundary conditions imposed until vaporization commences ($0 < t < t_v$) are

at $x = 0$

$$q_b = K_W \frac{\partial T}{\partial x} = 0^s$$

Thus

$$\frac{\partial T}{\partial x} = 0 \quad (2.14)$$

at $x = L$

$$q_0 = K_D \frac{\partial T}{\partial x} = \text{constant} \quad (2.15)$$

with the onset of vaporization ($t \geq t_v$) the slab is divided into two regions with the following conditions:

Wetted region ($0 \leq x \leq l$) at $x = 0$

$$q_b = K_W \frac{\partial T}{\partial x} = 0$$

or as above

$$\frac{\partial T}{\partial x} = 0$$

at $x = l$

$$T(x,t) = T_v = \text{constant} \quad (2.16)$$

^s The signs of q_b and q_0 are negative as a result of the problem being oriented in the negative x direction.

Dry region ($l \leq x \leq L$) at $x = l$

$$T(x,t) = T_v = \text{constant}$$

at $x = L$

$$q_0 = k_D \frac{\partial T}{\partial x} = \text{constant}$$

The boundary conditions (2.14) and (2.15) with respect to the front and back surfaces, therefore remain throughout the entire process with the addition of a third condition (2.16) when vaporization begins. The complete problem is thus defined by equations (2.6), (2.8) and (2.9) with initial conditions (2.10) through (2.13) and boundary conditions (2.14) through (2.16) for all time $t \geq 0$. The assumptions made thus far can be summarized as follows: A constant, radiative heat flux was applied to a semi-infinite slab. No ignition or chemical reaction of the slab was considered. The slab was divided into two regions by the vaporization interface. The changes in potential and kinetic energies were neglected in the application of the first law of thermodynamics to each region and at the vaporization interface. Work done on the fluid by viscous forces was neglected. The internal energy was assumed to be a function of temperature only. The mass flow rate of the fluid entering the moving vaporization interface was assumed equal to the mass flow of the vapor leaving. Within the vaporization interface the temperature and the densities of the liquid and vapor were considered constant. The dry region was considered as an infinite sink with respect to the vapor. Therefore the heat capacity of the vapor and the thermal energy convected away from the solid as a result of the flow of vapor through it were eliminated from the energy equation of the dry region.

Non-Dimensionalization

All variables in the aforementioned equations and conditions may be non-dimensionalized by some chosen characteristic dimension of the problem. The analysis is thus freed of dimensional dependency and allows the problem to be specified by relatively few pertinent parameters. The independent variable x and the dependent variable $l(t)$ are non-dimensionalized by the characteristic length L (slab thickness). The independent variable t (time) is non-dimensionalized by the characteristic conduction time L^2/α to yield the Fourier number. The temperature, measured from some reference temperature T_R , is made dimensionless by considering the boundary conditions at the front and back surfaces. The remaining variables are rendered dimensionless after division by their initial values. Table I presents a list of the resulting non-dimensional variables.

When the non-dimensional variables are substituted into the energy equations (2.6), (2.8) and (2.9) and the boundary conditions (2.14) through (2.16) it is possible to form dimensionless groups which simplify computation.⁴ The new parameters thus formed are used to characterize the solution of the problem in place of the non-dimensional variables separately. These incurred parameters are given in Table II.

The resulting non-dimensional energy equations are;

$$\begin{aligned} & \text{wetted region } (0 \leq \bar{x} < \bar{l}(\bar{t}_W)) \\ & \frac{\partial \bar{T}(\bar{x}, \bar{t}_W)}{\partial \bar{t}_W} = \frac{\partial^2 \bar{T}(\bar{x}, \bar{t}_W)}{\partial \bar{x}^2} \end{aligned} \quad (2.17)$$

⁴ See Appendix B.

TABLE I

NON-DIMENSIONAL VARIABLES

Dependent	Independent
$\bar{T}(\bar{x}, \bar{t}_W) = \frac{T_A - T_R}{q_o L / K_W}$	$\bar{x} = \frac{x}{L}$
$\bar{l}(\bar{t}_W) = \frac{l(t)}{L}$	$\bar{t}_W = \frac{\alpha_W t}{L^2}$
$\bar{\rho}_W(\bar{x}, \bar{t}_W) = \frac{\rho_W(x, t)}{\rho_W(x, 0)}$	
$\bar{\rho}_D(\bar{x}, \bar{t}_W) = \frac{\rho_D(x, t)}{\rho_W(x, 0)}$	

TABLE II

NON-DIMENSIONAL PARAMETERS

$\bar{H} = \frac{h_{fg} \rho_l \alpha_W}{q_o L}$
$\bar{K} = \frac{K_D}{K_W}$
$\bar{A} = \frac{\alpha_D}{\alpha_W} = \frac{K_D}{K_W} \frac{\rho_W C_W}{\rho_D C_D} = \bar{K} \frac{\rho_W C_W}{\rho_D C_D}$

dry region ($\bar{l}(\bar{t}_W) < \bar{x} \leq 1$)

$$\frac{\partial \bar{T}(\bar{x}, \bar{t}_W)}{\partial \bar{t}_W} + \frac{\bar{T}(\bar{x}, \bar{t}_W)}{\bar{\rho}_D(\bar{x}, \bar{t}_W)} \frac{\partial \rho_D(\bar{x}, \bar{t}_W)}{\partial \bar{t}_W} = \frac{A}{\bar{A}} \frac{\partial^2 \bar{T}(\bar{x}, \bar{t}_W)}{\partial \bar{x}^2} \quad (2.18)$$

liquid-vapor interface ($\bar{x} = \bar{l}(\bar{t}_W)$)

$$\bar{H} \frac{d\bar{l}(\bar{t}_W)}{d\bar{t}_W} = \frac{\partial \bar{T}(\bar{x}, \bar{t}_W)}{\partial \bar{x}} \Big|_{\bar{l}^-} - \bar{K} \frac{\partial \bar{T}(\bar{x}, \bar{t}_W)}{\partial \bar{x}} \Big|_{\bar{l}^+} \quad (2.19)$$

The non-dimensional initial conditions become

$$\bar{T}(\bar{x}, 0) = 0 \quad (2.20)$$

$$\bar{C}_D \bar{\rho}_D(\bar{x}, 0) = \frac{C_D \rho_D(x, 0)}{C_W \rho_W(x, 0)} \quad (2.21)$$

$$\bar{C}_W \bar{\rho}_W(\bar{x}, 0) = 1 \quad (2.22)$$

$$\bar{\rho}_1(\bar{x}, 0) = \frac{\rho_1(x, 0)}{\rho_W(x, 0)} = 0 \quad (2.23)$$

with the non-dimensional boundary conditions

$$\frac{\partial \bar{T}(\bar{x}, \bar{t}_W)}{\partial \bar{x}} \Big|_{\bar{x}=0} = 0 \quad (2.24)$$

$$\frac{\partial \bar{T}(\bar{x}, \bar{t}_W)}{\partial \bar{x}} \Big|_{\bar{x}=1} = 1 \quad (2.25)$$

$$\bar{T}(\bar{x}, \bar{t}_W) \Big|_{\bar{x}=\bar{l}(\bar{t}_W)} = \bar{T}_V \quad (2.26)$$

CHAPTER III

MATHEMATICAL SOLUTION

Background

Except in limiting cases non-linear partial differential equations are not readily amenable to solution by analytic means. Complicated geometries, boundary conditions or laborious calculations lead to the use of the digital computer to calculate approximate solutions by numerical methods. Most methods of solution either approximate the derivatives and solve the resulting system of algebraic equations or reduce the non-linear partial differential equations to linear ordinary differential equations and integrate this resulting set of equations by some method of numerical quadrature.

The finite-difference approach is used quite extensively in the solution of boundary value problems. The derivatives are approximated at given nodal points by various difference schemes, many of which are described by Özisik (18). The resulting system of algebraic equations must be solved at each step (increment of the independent variable), which becomes cumbersome when many equations are involved requiring considerable amounts of core storage and computational time. The repeated solution of these equations over a period of time may lead to an accumulative round-off error within the order of magnitude of the coefficients involved. The accuracy of the finite-difference method is controlled by the number of nodal points, or the grid spacing chosen.

Therefore, as accuracy is increased, computer storage, execution time, and possibly round-off error are increased.

With the development of highly sophisticated computer routines for the simultaneous integration of ordinary differential equations, the integral method, in which partial differential equations are reduced to ordinary differential equations, has become quite popular. The method of integral relations described by Belotserkovskii and Chushkin (4) and the procedure used by Goodman and Shea (10) to obtain their heat balance integral are two examples of the integral method. Basically, the partial differential equation is multiplied by a weighting function of the spacial coordinate and then integrated with respect to this variable. The remaining functions within the integrals are then approximated by some interpolation formula. The integrals are then evaluated and the resulting system of ordinary differential equations can be integrated by any number of numerical methods. Care must be taken in the selection of the formulas used to approximate these integrals (e.g. polynomials, spline functions, trigonometric series, geometric series). If a polynomial is chosen, the ordinary differential equation which results will be dependent on the selection of nodes with respect to the spacial coordinate much like the finite-difference method. Also at each step, simultaneous algebraic equations must be solved where in some cases, (i.e. coefficients with very small values) the accumulation of round-off error or the singularity of a matrix will lead to unpredictable integration results.

Some numerical methods for integrating ordinary differential equations incorporate a weighting function (chosen by the user) which is a factor in determining the accuracy of each integration step.

Therefore, if the weighting function utilized in reducing the partial differential equation weights certain areas of the problem for higher accuracy, care must be taken in applying integration methods to avoid additive or canceling weights.

The dependence on nodal selective and possible additive round-off errors can be eliminated by electing the weighting function and the approximation function to be orthogonal. The calculations required to solve the problem are also reduced since the integral of the product of two orthogonal functions, i.e.

$$\int_a^b f_m(x) g_n(x)$$

is zero except when m and n are equal. With the proper choice of functions, the heat conduction equation is transformed into an equation satisfying the original only approximately. This technique or the weak solution is employed in this study.

The extension of the Schmidt graphical method of solution suggested by Longwell (13), while of interest, is tedious and its accuracy depends on the exactness of construction. This method can be used, however, to show trends and gross effects within the magnitude of more detailed solutions if so desired.

Application of the Integral Method

The primary concern of this study is the first of the limiting cases discussed in Chapter I. Accordingly the following equations are considered:

equation (2.17)

$$\frac{\lambda \bar{T}(\bar{x}, \bar{t}_W)}{\partial \bar{t}_W} = \frac{\partial^2 \bar{T}(\bar{x}, \bar{t}_W)}{\partial \bar{x}^2}$$

equation (2.18) minus the energy generation or absorption term

$$\frac{\lambda \bar{T}(\bar{x}, \bar{t}_W)}{\partial \bar{t}_W} = \bar{A} \frac{\partial^2 \bar{T}(\bar{x}, \bar{t}_W)}{\partial \bar{x}^2}$$

and equation (2.19)

$$\bar{H} \frac{d\bar{l}(\bar{t}_W)}{d\bar{t}_W} = \frac{\partial \bar{T}(\bar{x}, \bar{t}_W)}{\partial \bar{x}} \Big|_{\bar{l}^-} - \bar{K} \frac{\partial \bar{T}(\bar{x}, \bar{t}_W)}{\partial \bar{x}} \Big|_{\bar{l}^+}$$

\bar{A} and \bar{K} are given in Table II.

Solving for $\bar{t}_W > \bar{t}_v$ (after vaporization commences) equation (2.17) is multiplied by the weighting function $Q(\bar{x})$ and integrated with respect to \bar{x} over the interval $[0, \bar{l}]$

$$\int_0^{\bar{l}(\bar{t}_W)} Q(\bar{x}) \frac{\partial \bar{T}(\bar{x}, \bar{t}_W)}{\partial \bar{t}_W} d\bar{x} = \int_0^{\bar{l}(\bar{t}_W)} Q(\bar{x}) \frac{\partial^2 \bar{T}(\bar{x}, \bar{t}_W)}{\partial \bar{x}^2} d\bar{x} \quad (3.1)$$

Applying Leibnitz's formula for differentiating an integral and integration by parts yields ⁵

⁵ See Appendix C.

$$\begin{aligned}
& \frac{d}{d\bar{t}_W} \int_0^{\bar{l}(\bar{t}_W)} Q(\bar{x}) \bar{T}(\bar{x}, \bar{t}_W) d\bar{x} - Q(\bar{x}) \bar{T}(\bar{x}, \bar{t}_W) \frac{\partial \bar{l}(\bar{t}_W)}{\partial \bar{t}_W} \Big|_{\bar{x}=\bar{l}} = \\
& Q(\bar{x}) \frac{\partial \bar{T}(\bar{x}, \bar{t}_W)}{\partial \bar{x}} \Big|_0^{\bar{l}(\bar{t}_W)} - Q'(\bar{x}) \bar{T}(\bar{x}, \bar{t}_W) \Big|_0^{\bar{l}(\bar{t}_W)} \\
& + \int_0^{\bar{l}(\bar{t}_W)} Q''(\bar{x}) \bar{T}(\bar{x}, \bar{t}_W) d\bar{x} \tag{3.2}
\end{aligned}$$

Similarly multiplying equation (2.18) by $Q(\bar{x})$ and integrating with respect to \bar{x} over the interval $[\bar{l}, 1]$.

$$\int_{\bar{l}(\bar{t}_W)}^1 Q(\bar{x}) \frac{\partial \bar{T}(\bar{x}, \bar{t}_W)}{\partial \bar{t}_W} d\bar{x} = \bar{A} \int_{\bar{l}(\bar{t}_W)}^1 Q(\bar{x}) \frac{\partial^2 \bar{T}(\bar{x}, \bar{t}_W)}{\partial \bar{x}^2} d\bar{x} \tag{3.3}$$

Applying Leibnitz's formula for differentiating an integral and integrating by parts yields⁶

$$\begin{aligned}
& \frac{d}{d\bar{t}_W} \int_0^1 Q(\bar{x}) \bar{T}(\bar{x}, \bar{t}_W) d\bar{x} + Q(\bar{x}) \bar{T}(\bar{x}, \bar{t}_W) \frac{\partial \bar{l}(\bar{t}_W)}{\partial \bar{t}_W} \Big|_{\bar{x}=\bar{l}(\bar{t}_W)} = \\
& \bar{A} Q(\bar{x}) \frac{\partial \bar{T}(\bar{x}, \bar{t}_W)}{\partial \bar{x}} \Big|_{\bar{l}(\bar{t}_W)}^1 - \bar{A} Q'(\bar{x}) \bar{T}(\bar{x}, \bar{t}_W) \Big|_{\bar{l}(\bar{t}_W)}^1 \\
& + \bar{A} \int_{\bar{l}(\bar{t}_W)}^1 Q''(\bar{x}) \bar{T}(\bar{x}, \bar{t}_W) d\bar{x} \tag{3.4}
\end{aligned}$$

⁶ See Appendix D.

To obtain the integral over the entire slab $[0,1]$ equations (3,2) and (3.4) are added to produce when further simplified,

$$\begin{aligned}
\frac{d}{d\bar{t}_W} \int_0^1 Q(\bar{x}) \bar{T}(\bar{x}, \bar{t}_W) d\bar{x} &= Q(\bar{x}) \frac{\partial \bar{T}(\bar{x}, \bar{t}_W)}{\partial \bar{x}} \Big|_{\bar{x}=\bar{\ell}^-} && \text{I} \\
- \bar{A} Q(\bar{x}) \frac{\partial \bar{T}(\bar{x}, \bar{t}_W)}{\partial \bar{x}} \Big|_{\bar{x}=\bar{\ell}^+} &- Q(\bar{x}) \frac{\partial \bar{T}(\bar{x}, \bar{t}_W)}{\partial \bar{x}} \Big|_{\bar{x}=0} && \text{II, III} \\
+ \bar{A} Q(\bar{x}) \frac{\partial \bar{T}(\bar{x}, \bar{t}_W)}{\partial \bar{x}} \Big|_{\bar{x}=1} &- Q'(\bar{x}) \bar{T}(\bar{x}, \bar{t}_W) \Big|_{\bar{x}=\bar{\ell}} && \text{IV, V} \\
+ Q'(\bar{x}) \bar{T}(\bar{x}, \bar{t}_W) \Big|_{\bar{x}=0} &- \bar{A} Q'(\bar{x}) \bar{T}(\bar{x}, \bar{t}_W) \Big|_{\bar{x}=1} && \text{VI, VII} \\
+ \bar{A} Q'(\bar{x}) \bar{T}(\bar{x}, \bar{t}_W) \Big|_{\bar{x}=\bar{\ell}} &&& \text{VIII} \\
+ \int_0^{\bar{\ell}(\bar{t}_W)} Q''(\bar{x}) \bar{T}(\bar{x}, \bar{t}_W) d\bar{x} &+ \int_{\bar{\ell}(\bar{t}_W)}^1 Q''(\bar{x}) \bar{T}(\bar{x}, \bar{t}_W) d\bar{x} && \text{IX, X}
\end{aligned} \tag{3.5}$$

Term I is the heat flux exiting the interface in the -x direction and

Term II is the heat flux entering the interface in the -x direction.

In this initial study for simplification \bar{A} and \bar{K} are chosen to be unity and equation (2,19) can be substituted for Terms I and II. Terms V and VIII will then add out and the resulting equation is

$$\begin{aligned}
\frac{d}{d\bar{t}_W} \int_0^1 Q(\bar{x}) \bar{T}(\bar{x}, \bar{t}_W) d\bar{x} &= Q(\bar{x}) \bar{H} \frac{d\bar{l}(\bar{t}_W)}{d\bar{t}_W} \\
&\quad \text{I} \\
&\quad - Q(\bar{x}) \left. \frac{\partial \bar{T}(\bar{x}, \bar{t}_W)}{\partial \bar{x}} \right|_{\bar{x}=0} + Q(\bar{x}) \left. \frac{\partial \bar{T}(\bar{x}, \bar{t}_W)}{\partial \bar{x}} \right|_{\bar{x}=1} \\
&\quad \text{II} \qquad \qquad \qquad \text{III} \\
&\quad + Q'(\bar{x}) \bar{T}(\bar{x}, \bar{t}_W) \Big|_{\bar{x}=0} - Q'(\bar{x}) \bar{T}(\bar{x}, \bar{t}_W) \Big|_{\bar{x}=1} \\
&\quad \text{IV} \qquad \qquad \qquad \text{V} \\
&\quad + \int_0^1 Q''(\bar{x}) \bar{T}(\bar{x}, \bar{t}_W) d\bar{x} \qquad \qquad \qquad (3.6) \\
&\quad \text{VI}
\end{aligned}$$

Substituting boundary conditions (2.24) and (2.25) into Terms II and III respectively, and rearranging

$$\begin{aligned}
\frac{d}{d\bar{t}_W} \int_0^1 Q(\bar{x}) \bar{T}(\bar{x}, \bar{t}_W) d\bar{x} &= Q(\bar{x}) \bar{H} \frac{d\bar{l}(\bar{t}_W)}{d\bar{t}_W} \\
&\quad - Q(\bar{x}) (0) + Q(\bar{x}) (1) + Q'(\bar{x}) \bar{T}(0, \bar{t}_W) - Q'(\bar{x}) \bar{T}(1, \bar{t}_W) \\
&\quad + \int_0^1 Q''(\bar{x}) \bar{T}(\bar{x}, \bar{t}_W) d\bar{x} \qquad \qquad \qquad (3.7) \\
&\quad 0
\end{aligned}$$

The functions chosen for the weighting function ($Q(\bar{x})$) and the temperature approximation function ($\bar{T}(\bar{x}, \bar{t}_W)$) must be continuous, complete and have at least continuous second derivatives on the interval of interest ($0 \leq \bar{x} \leq 1$). Equation (3.7) is void of all derivatives of temperature with respect to \bar{x} . The discontinuity of this derivative of temperature at the interface was removed by substitution of equation (2.19). Thus the weighting and approximation functions are not required to satisfy the derivative of temperature with respect to \bar{x} . The temperature

throughout the slab and at the boundaries is then the primary requirement which these functions must satisfy. The cosine function (i.e. $\cos n\pi\bar{x}$) is chosen for two reasons. First, $\cos n\pi\bar{x}$ exists within the region $0 < \bar{x} < 1$ and at the boundaries of the semi-infinite slab ($\bar{x} = 0, 1$), therefore, the temperature requirement is satisfied. Secondly, the cosine function ($\cos n\pi\bar{x}$) is orthogonal with respect to itself which greatly reduces computations. The derivative of $\cos n\pi\bar{x}$ matches the boundary condition at the back wall (2.24) but does not match the boundary condition at the surface (2.25). Again this is of no consequence since the boundary conditions (2.24) and (2.25) along with equation (2.19) are substituted into the energy equation (3.6) thus eliminating all derivatives of temperature with respect to \bar{x} .

Choosing then the weighting function $Q(\bar{x})$ to be

$$Q(\bar{x}) = \cos m\pi\bar{x} \quad m = 0, 1, 2, \dots, N \quad (3.8)$$

and approximating the temperature by

$$\bar{T}(\bar{x}, \bar{t}_W) = \sum_{n=0}^N A_n(\bar{t}_W) \cos n\pi\bar{x} \quad n = 0, 1, 2, \dots, N \quad (3.9)$$

equation (3.7) produces N equations of the form⁷

$$\begin{aligned} \frac{dA_n(\bar{t}_W)}{d\bar{t}_W} &= 2 \cos(n\pi\bar{l}) \bar{H} \frac{d\bar{l}(\bar{t}_W)}{d\bar{t}_W} + 2 \cos(n\pi) \\ &\quad - (n\pi)^2 A_n(\bar{t}_W) \quad (n > 0) \end{aligned} \quad (3.10)$$

and for $n = 0$

$$\frac{dA_0(\bar{t}_W)}{d\bar{t}_W} = \bar{H} \frac{d\bar{l}(\bar{t}_W)}{d\bar{t}_W} + 1 \quad (3.11)$$

⁷ See Appendix E.

In deriving the (N+1) equations (3.10) and (3.11) above, equations (2.17) through (2.19) were used with boundary conditions (2.24) and (2.25). The remaining condition at the interface ($\bar{x} = \bar{\ell}(\bar{t}_W)$) is boundary condition (2.26).

$$\bar{T}(\bar{\ell}, \bar{t}_W) = \bar{T}_V = \text{constant}$$

The total derivative of \bar{T}_V is zero. Then

$$d\bar{T}_V = 0 = \left. \frac{\partial \bar{T}_V}{\partial \bar{t}_W} \right)_{\bar{x}} d\bar{t}_W + \left. \frac{\partial \bar{T}_V}{\partial \bar{x}} \right)_{\bar{t}_W} d\bar{x}$$

By equation (3.9)

$$\bar{T}_V = \sum_{n=0}^N A_n(\bar{t}_W) \cos(n\pi \bar{\ell})$$

Therefore, the additional equation produced becomes

$$0 = \sum_{j=0}^N \frac{dA_j(\bar{t}_W)}{d\bar{t}_W} \cos(j\pi \bar{\ell}) - \frac{d\bar{\ell}(\bar{t}_W)}{d\bar{t}_W} \sum_{j=0}^N (j\pi) A_j(\bar{t}_W) \sin(j\pi \bar{\ell}) \quad j = 0, 1, 2, \dots, N \quad (3.12)$$

This yields (N+2) equations with (N+2) unknowns. The problem is reduced then to the simultaneous solution of equations (3.10) through (3.12) to obtain values of

$$\frac{dA_j}{d\bar{t}_W} \quad j = 0, 1, 2, \dots, N$$

then integrating these values with respect to time by some numerical method resulting in the N+1 coefficients A_j , $j = 0, 1, 2, \dots, N$.

As a consequence of utilizing orthogonal functions the set of N+2 simultaneous algebraic equations (3.10) through (3.12) may be solved

once for all time. Thereby the need to solve this set of equations simultaneously at each step in the problem solution is eliminated. Solving for the derivative of the interface location with respect to time yields⁸

$$\frac{d\bar{l}(\bar{t}_W)}{d\bar{t}_W} = - \frac{\left\{ 1+2 \sum_{j=1}^N [\cos(j\pi) \cos(j\pi\bar{l})] \right\} - \sum_{j=1}^N (j\pi)^2 A_j \cos(j\pi\bar{l})}{\left\{ 1+2 \sum_{j=1}^N \cos^2(j\pi\bar{l}) \right\} - \sum_{j=1}^N (j\pi) A_j \sin(j\pi\bar{l})} \quad (3.13)$$

Substituting the solution of equation (3.13) into equations (3.10) and (3.11) at each step will yield the values of the coefficient derivatives

$$\frac{dA_j(\bar{t}_W)}{d\bar{t}_W} \quad j = 0, 1, 2, \dots, N$$

to be integrated.

The solution of the problem before vaporization (i.e. $\bar{l} = 1$) can be accomplished analytically.

For $0 < \bar{t}_W < \bar{t}_V$, $\bar{l} = 1 = \text{constant}$

$$\frac{d\bar{l}}{d\bar{t}_W} = 0$$

Equation (3.10) reduces to

$$\frac{dA_n(\bar{t}_W)}{d\bar{t}_W} = 2 \cos(n\pi) - (n\pi)^2 A_n(\bar{t}_W) \quad (3.14)$$

for $n > 0$, with equation (3.11) being

$$\frac{dA_0(\bar{t}_W)}{d\bar{t}_W} = 1 \quad (3.15)$$

⁸ See Appendix F.

Integrating equations (3.14) and (3.15) results in⁹

$$A_0(\bar{t}_W) = \bar{t}_W \quad (3.16)$$

$$A_n(\bar{t}_W) = \frac{2(-1)^n}{(n\pi)^2} \left[\exp \{ - (n\pi)^2 \bar{t}_W \} - 1 \right] \quad (n > 0) \quad (3.17)$$

The problem is therefore solved algebraically for any increment of time between zero and the time vaporization commences at the front surface (i.e. $0 < \bar{t}_W < \bar{t}_v$),

Initial Conditions

Of the non-dimensional initial conditions given in Chapter II, only condition (2.20) is pertinent to the vaporization study.

At $\bar{t}_W = 0$, condition (2.20) states

$$\bar{T}(\bar{x}, 0) = 0$$

Applying the temperature approximation (3.9) to condition (2.20) yields

$$\bar{T}(\bar{x}, 0) = \sum_{n=0}^N A_n(0) \cos(n\pi\bar{x}) \quad n = 0, 1, 2, \dots, N$$

$\cos(n\pi\bar{x})$ will be zero for $\bar{x} = \frac{1}{2}$ only. Therefore $A_n(0)$ must be zero.

The initial temperature coefficients are then

$$\begin{aligned} A_0 &= 0 \\ A_1 &= 0 \\ &\cdot \\ &\cdot \\ A_N &= 0 \end{aligned}$$

⁹ See Appendix G,

Computer Technique

The computer program developed to solve the first case or vaporization problem described by equations (3.10) through (3.17) consists of four sections or subroutines. The main or executive section (MAIN) initiates all control parameters, non-dimensional parameters, and equation coefficients. This section solves the algebraic equations (3.16) and (3.17) for the heating of the saturated porous slab prior to vaporization (i.e. $0 < \bar{t}_W < \bar{t}_V$) and initiates the integration of equations (3.10), (3.11), and (3.13).

The output section (DEROUT) prints and/or punches any desired temperatures along with the vaporization position and velocity for various increments of time.

The derivative function subroutine (DERFUN) calculates the derivatives of the coefficients, using equations (3.10), (3.11), and (3.13) for each successive time step employing previous values of the coefficients obtained from the integration routine.

The integration routine (DHPCG) integrates the calculated values of the derivatives given by the derivative function and passes the new values of the coefficients to the output and derivative function routines. A complete listing of each program section is given in Appendix I. Table III presents the basic steps followed by the computer program.

Method of Numerical Integration

Numerical techniques for solving first order ordinary differential equations with given conditions $y_i(x_0)$ are usually based on the direct or indirect use of Taylor's expansion or on the employment of open or

TABLE III
COMPUTER PROGRAM CYCLE

I. Main Section

1. Read summation limit (N), dimensional constants, output and integration routine control parameters.
2. Initialize numerical constants and non-dimensional parameters.
3. Calculate coefficients for the temperature approximation function by the analytic solution ($0 < \bar{t}_W < \bar{t}_V$). Call output routine.
4. Repeat step 3 until vaporization commences ($\bar{t}_W = \bar{t}_V$).
5. Initialize constants required for numerical integration.
6. Call integration routine (II).

II. Integration Routine

1. Apply one-step integration method.
2. Call derivative function and output routines.
3. Apply multistep integration method.
4. Call derivative function (III) and output (IV) routines.
5. Repeat steps 3 and 4 until the entire interval specified is integrated over or an unresolvable error is encountered.
6. Return to main section (I).

III. Derivative Function Routine

1. Using coefficient values received from the integration routine (II) calculate the temperature coefficient derivatives for the next integration step.

TABLE III (Continued)

-
2. Return to the integration routine (II).

IV. Output Routine

1. Determine if output is desired for this step.
 2. Calculate temperatures at specified locations throughout slab.
 3. Determine when vaporization begins.
 4. Print or punch time, interface velocity, interface position and desired temperature profiles.
 5. Return to calling routine.
-

closed integration formulas. Carnahan, Luther, and Wildes (7) group these techniques into two classes, one-step methods which calculate the value y_{i+1} given only y_i and the multistep methods requiring y_i plus several other values y_i 's outside the integral of integration.

One disadvantage of the multistep methods is that they are not self-starting and require a one-step method to calculate the initial values of the solution y_i (i.e., $y(x_1)$, $y(x_2)$, etc.). Also with multistep methods it is cumbersome to change the integration step size once the calculation is initiated. The major advantage of multistep methods is the fact that less computation is required than comparable one-step methods while producing results of similar accuracy.

The predictor-corrector methods, where an open integration formula is utilized to predict the integration and a closed integration formula is employed to correct this estimate, inherit the disadvantages of the multistep methods. But a considerable advantage of this method is that solutions can be produced with comparable accuracy and stability of a fourth order one-step method using as few as two derivative evaluations at each step. Hamming's modified predictor-corrector method represents the best compromise between stability and accuracy and is the most popular multistep method (7).

The numerical integration method used in this study is an IBM application program (DHPCL) (24) which employs Hamming's modified predictor-corrector method with a fourth order Runge-Kutta method, suggested by Ralston (20), to start the process. This routine incorporates an error weighting function and allows the user the option of changing the integration step size during execution.

CHAPTER IV

COMPUTATIONAL RESULTS

Inert Solution

By the nature of the problem presented in Chapters II and III, an algebraic solution is possible for the heating of the saturated porous slab from time zero till the time of vaporization at the front surface. To assess this analytic solution the condition of vaporization at the surface was relaxed and the problem became one of the heating of an inert slab. Carslaw and Jaeger (8) give the exact solution for an inert semi-infinite slab heated by a constant heat flux at the front surface with an adiabatic back surface.

Figure 6 presents a comparison of the computer generated approximate solution utilizing five coefficients with the exact solution. A good approximation at the front surface is obtained while the inert calculations match the exact solution precisely at the back surface. Increasingly the number of coefficients in the inert solution will cause the exact solution at the front surface to be more closely modeled.

Constant and Parameter Values

The dimensional constants in the series of computational runs discussed here, were chosen to match approximately those of wood and water. Since the examination of the entire problem will eventually encompass pyrolysis, the constants and parameters generally match those

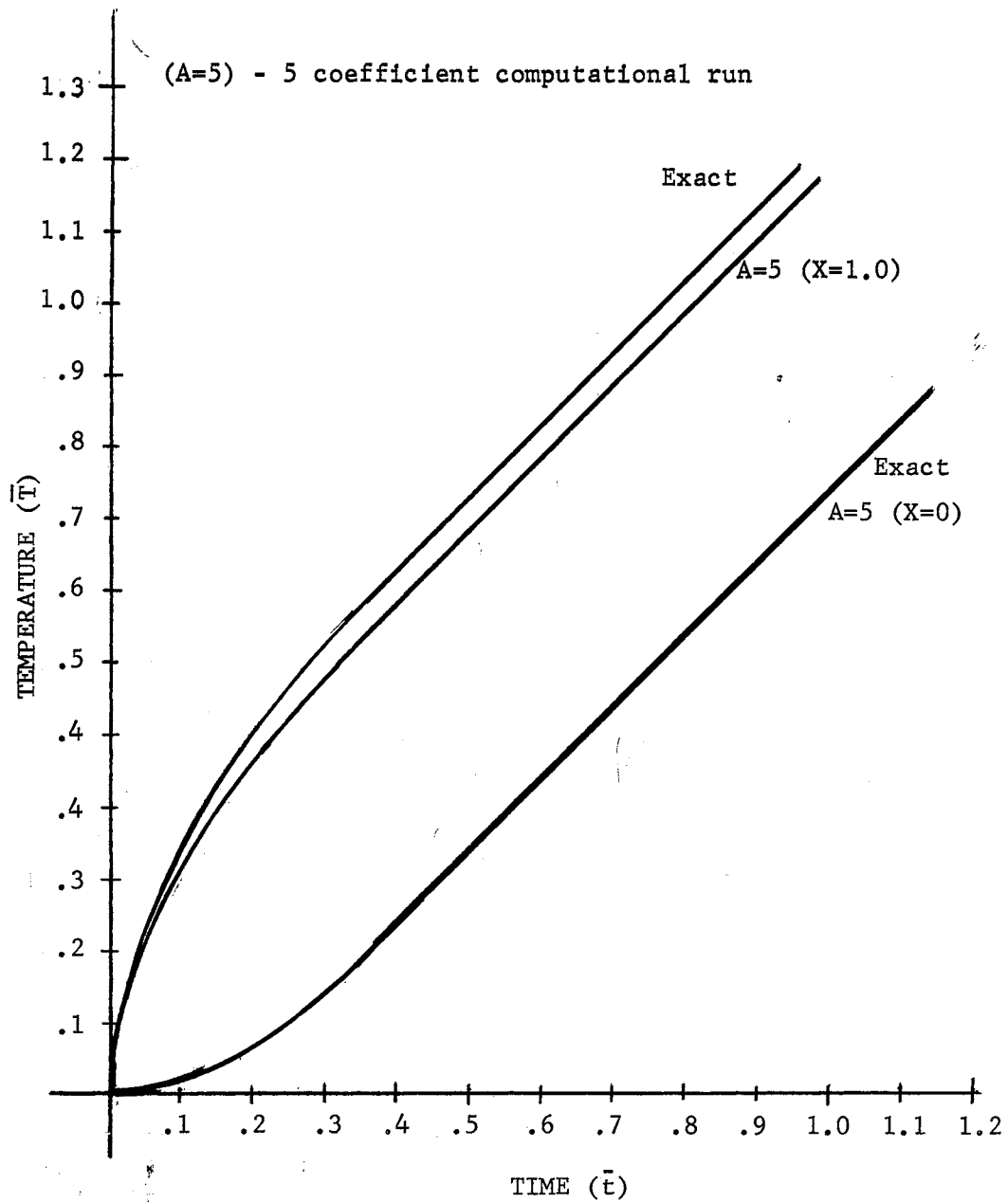


Figure 6. Comparison of Approximate Solution of Inert Slab With Exact Solution

of Rittmann (21) for future study. Table 4 lists the pertinent constants and parameters used.

Temperature Relations

Comparison of the temperatures obtained in this investigation with work previously done in the melting and freezing problem is difficult for two reasons. Firstly, the studies encountered consider the liquid or solid at a uniform temperature of solidification or melting before the process is initiated. Secondly, most previous studies use a step input of temperature to initiate the melting of solidification process. This study assumes the saturated slab is at a reference temperature well below that of vaporization and consequently when the constant heat flux is applied the temperature is no longer uniform throughout the slab. When vaporization commences the temperature profiles and the velocity of the interface are quite different than presented in other studies. Also the term containing the temperature at the front surface was deleted from the energy equation (3.7) as a result of the choice of cosine weighting and approximation functions. Therefore the application of a step input temperature is not possible.

A time history of temperatures at selected points within the slab is shown in Figure 7.¹⁰ By comparison with Figure 6, the inert solution, it can be seen that when the front surface reaches vaporization ($\bar{t}_W = .05937$) the temperature remains constant for some time. This is caused by the decrease in heat flux entering the remainder of the slab as a result of vaporization at and near the surface. The temperature

¹⁰The graphs presented have been smoothed over discrete points to eliminate cosine fluctuations.

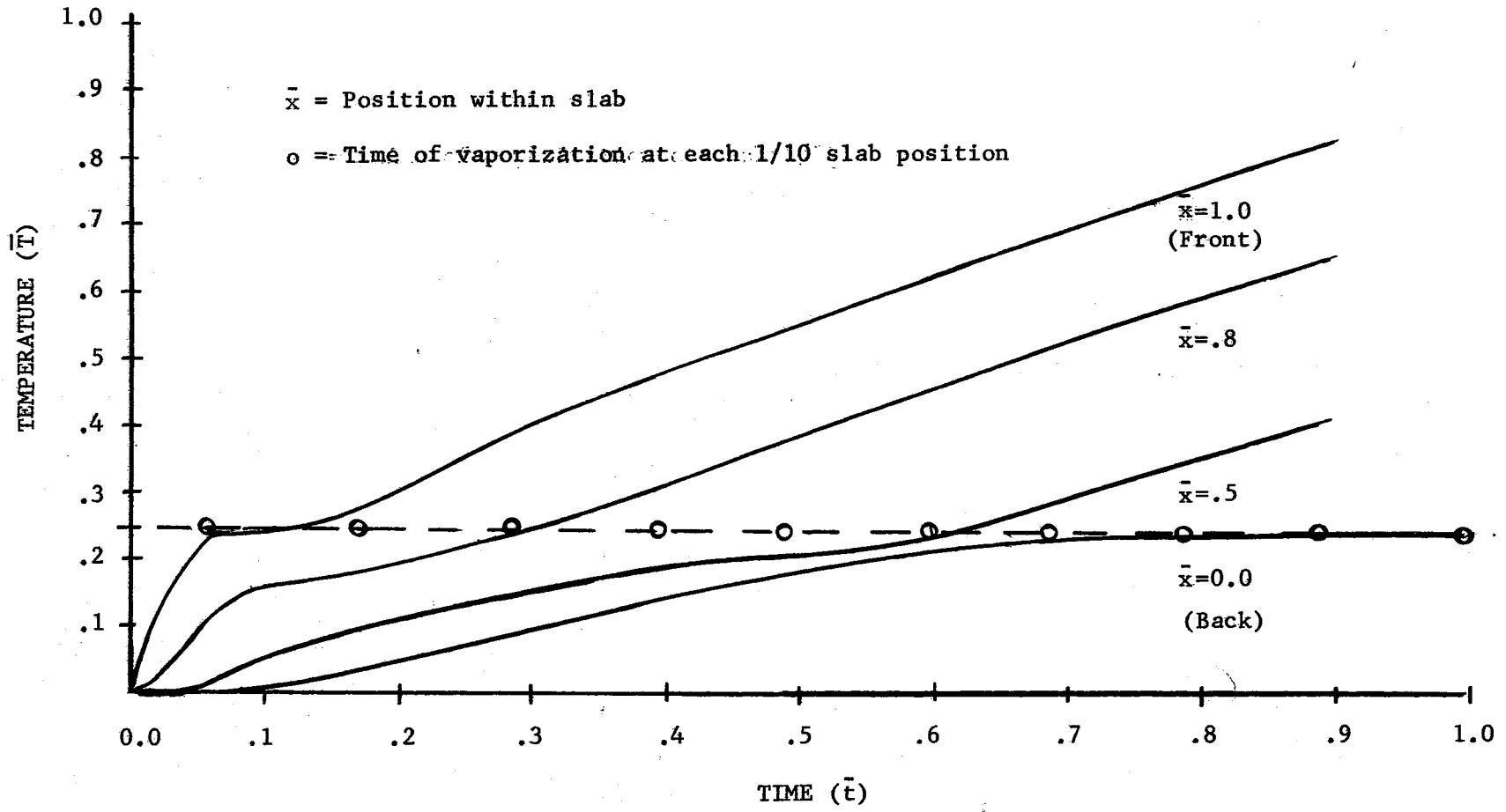


Figure 7. Selected Temperature Profiles With Respect to Time

TABLE IV
DIMENSIONAL CONSTANTS AND
PARAMETERS

L	1.0 cm
T_R	300° K
q_o	0.081 cal/cm ² -sec
h_{fg}	539.05 cal/gm
T_V	373.15° K
C_W	.66 cal/gm-° K
K_W	2.7×10^{-4} cal-cm/cm ² -sec ² -° K
\bar{T}_V	.24383
\bar{H}	.544495
$\bar{\rho}_l$.20
\bar{A}	1.0
\bar{K}	1.0

gradient throughout the slab is decreased as a result of the onset of vaporization. As time increases the points in the dry region, far enough from the interface, are no longer affected by the vaporization and approach a conduction dominated linear increase in temperature. The temperature at the back wall increases constantly throughout the entire process and has virtually reached the temperature of vaporization when the interface is at a point approximately .4 from the back wall.

The temperature profile through the slab at selected times is shown in Figure 8. Here again it can be seen that the temperatures in the area preceding the vaporization interface (i.e. wetted region) increase very slowly, but the temperatures within the area aft of the interface (i.e. dry region) are unaffected. The temperature gradient on the wetted side of the interface decreases with time and eventually reaches zero at the back surface (boundary condition). This is physically realistic since the wetted region slowly reaches the temperature of vaporization as the interface moves into the slab. Therefore, the temperature gradient is significant with the onset of vaporization and then must decrease as the temperature increases in the region ahead of the interface.

Interface Velocity

Figure 9 contains discrete points plotted from computational runs of five and seven coefficients. The oscillations observed are attributed to the representation of an infinite series, i.e.

$$\sum_{n=0}^{\infty} A_n \cos n\pi\bar{x}$$

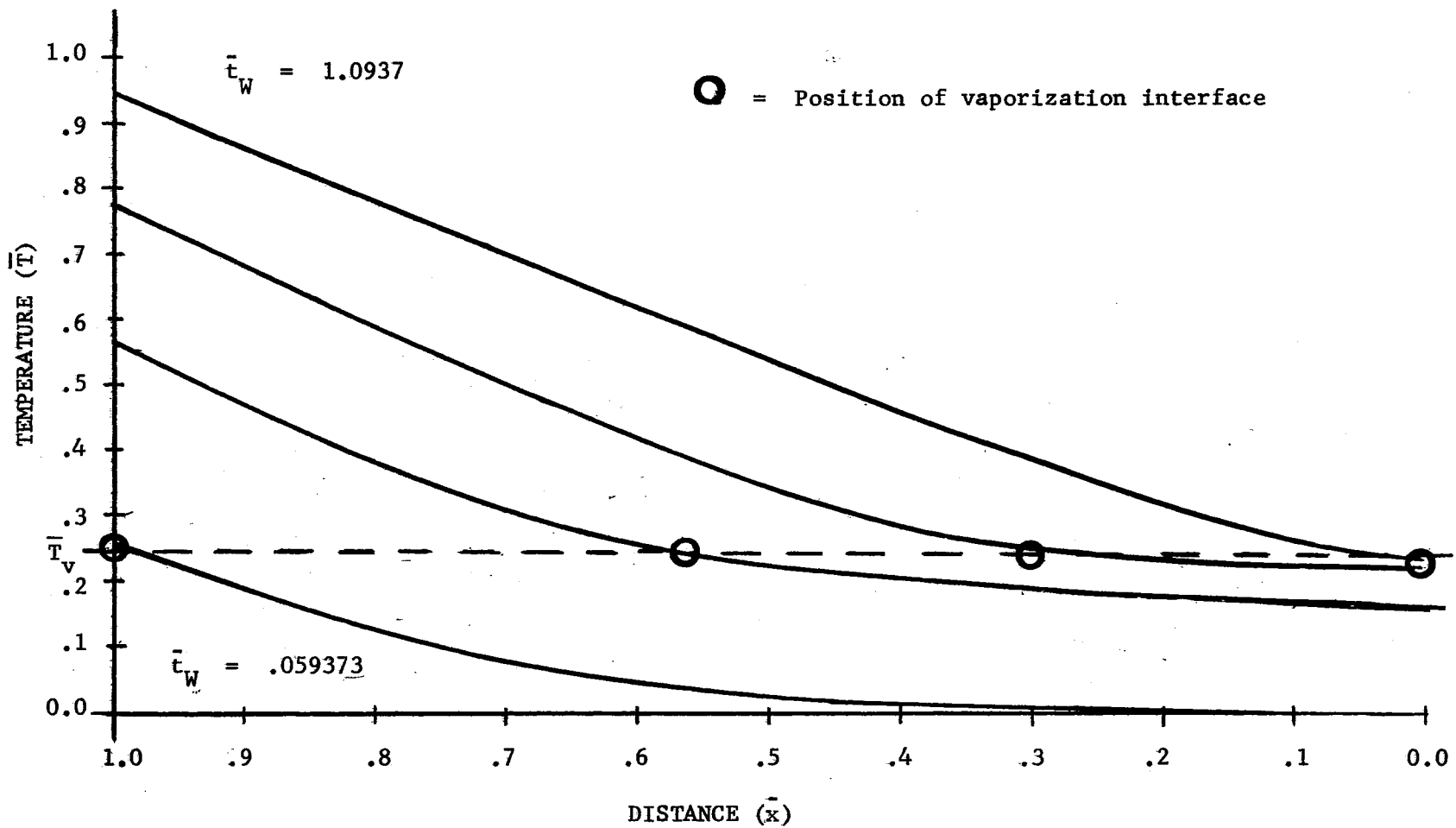


Figure 8. Temperature Profile of Slab at Selected Time Intervals

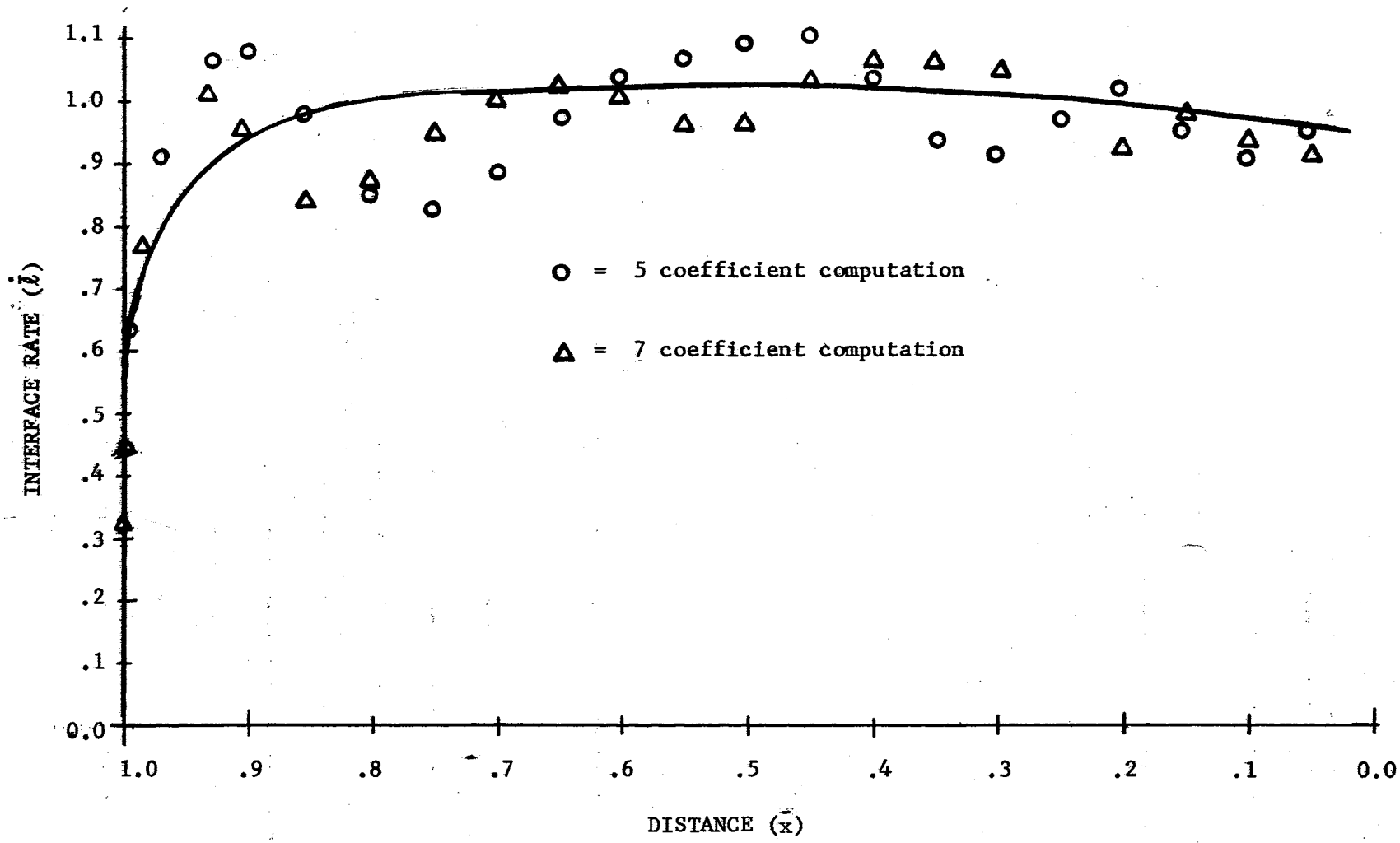


Figure 9. Interface Velocity With Respect to Distance

by a finite number of coefficients. Approximation of a mean value curve through these points shows the interface velocity starting at zero and rapidly increasing to a value in the neighborhood of .9. The velocity then increases slowly to a maximum somewhere in the vicinity of the center of the slab. From this point on the velocity drops off slowly through the remainder of the slab.

The interface velocity obtained appears to be physically realistic since at the onset of vaporization the surface and immediate area behind it are at the vaporization temperature. The rate of vaporization assumed starting at zero increases rapidly as the liquid in this area is vaporized. Once this initial area is vaporized a certain amount of flux must be used to heat the area immediately ahead of the interface to bring it to the temperature of vaporization. As the temperature in the wetted region increases the interface velocity increases slowly until a maximum is reached. At this point, the temperature gradient in the dry region is such that more and more energy is required in raising the temperature in this region. Thus the interface velocity decreases and continues decreasing throughout the remainder of the slab as the temperature gradient in the dry region increases.

The initial velocity as shown starts at definite rates of approximately .32 and .45. This is a consequence of the size of the initial integration step and also of the number of coefficients used.

Pyrolysis Retardation

Although the primary interest of this investigation is not pyrolysis, examination of Figure 10 reveals that, for a constant heat flux with one exothermic reaction considered, deviation from the inert

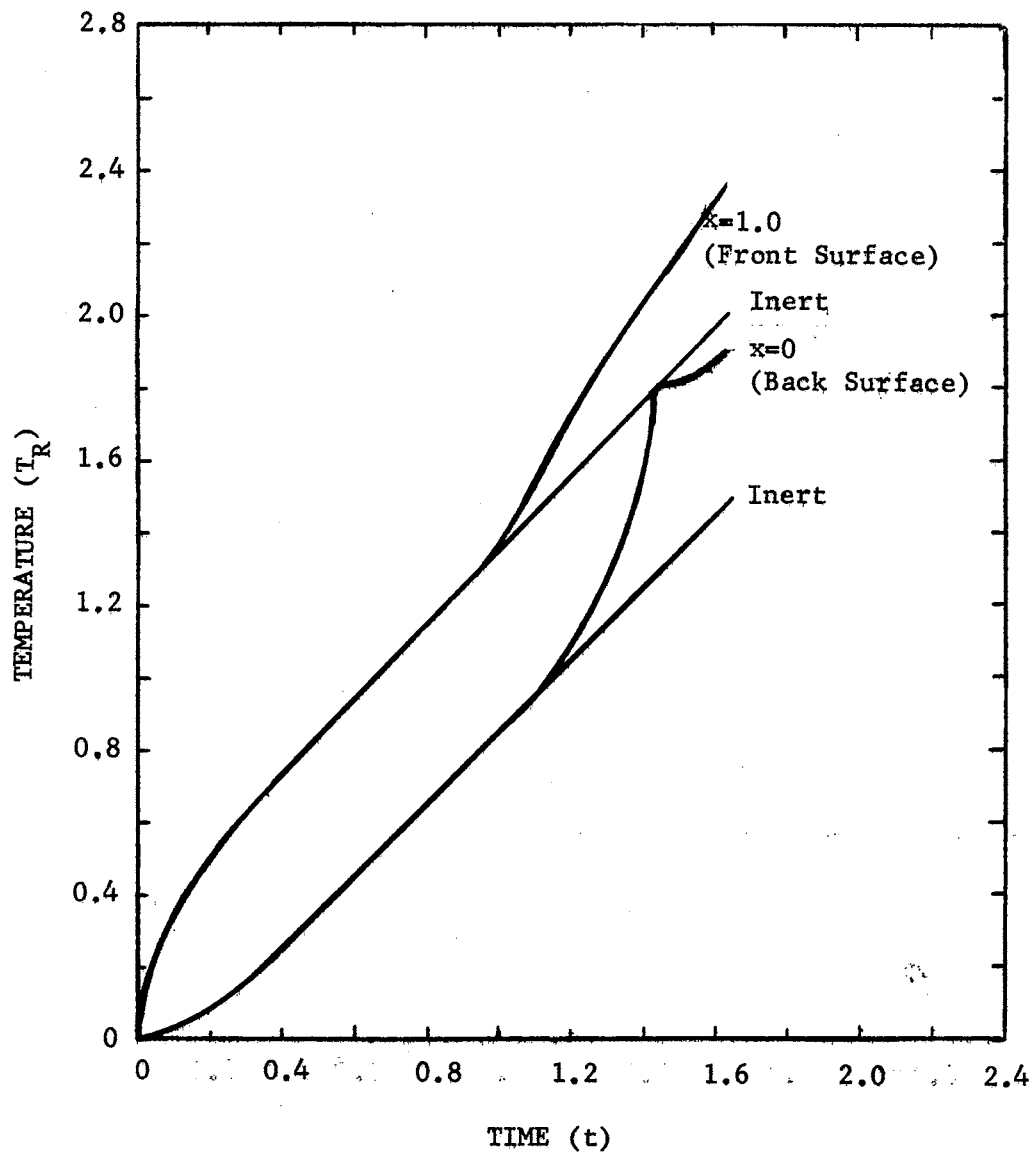


Figure 10. Effect of Heat of Reaction: Temperature History of Front and Back Surfaces - Constant Heat Flux, One Exothermic Reaction, Case 0, Rittmann (21)

solution occurs at a time of approximately $\bar{t}_W = .1$. The temperatures at this point for the front and back surfaces are $\bar{T} = 1.3$ and $\bar{T} = .9$, respectively. The seven coefficient computation utilized in Figures 7 and 8 obtained complete vaporization of the saturated liquid within a time a $\bar{t}_W = 1.094$. The maximum temperature attained by the front surface being $\bar{T} = .9312$ with the back surface restricted to $\bar{T} = .2438$ (i.e. The temperature of vaporization \bar{T}_V). Within the same time frame, (i.e. $0 \leq \bar{t}_W \leq 1.0$), comparison of the aforementioned figures discloses the temperature of the front surface in the saturated problem to be just slightly greater than that of the back surface of the pyrolysis example. Also, the back surface of the saturated problem is seen to be at a temperature much lower than the corresponding temperature of the pyrolysis problem. Thus, as expected, the dissipation of heat energy by vaporization of the liquid causes the temperatures within the initially saturated porous solid to be much lower than the temperatures of the initially dry heated solid thereby delaying pyrolysis of the solid material.

The solution of the vaporization problem presented here assumes thermal properties which yield values of the Fourier number and non-dimensional temperatures consistent with those used by Rittmann (21) in the calculation of various constant, radiative heat flux type pyrolysis problems. These values in no way attempt to model known substances. In Appendix H values of the non-dimensional parameters \bar{A} and \bar{K} are computed assuming water and fir are the substances used in a volumetric ratio of one to four. The values of \bar{A} and \bar{K} thus attained do not approach unity unless the ratio of liquid to solid is very small. Therefore, in future investigations the incorporation of these non-dimensional parameters

into the resultant energy equation must be resolved to extend this study to various combinations of known substances.

CHAPTER V

SUMMARY AND CONSLUSIONS

Summary

An analytic study of the heating of a porous material initially saturated with a liquid was undertaken. Examination of the complexity of the problem led to a division into two areas of analysis, the vaporization of the liquid and the pyrolysis of the porous material. This study concentrated on the phenomena of vaporization.

The vaporization of the liquid from a saturated porous solid was modeled by a semi-infinite, homogeneous and isotropic slab initially saturated with a homogeneous and isotropic liquid. The slab was considered exposed to a constant, radiative heat flux at the front surface and insulated against heat conduction at the back surface. With the onset of vaporization the slab was divided into two regions by the vaporization interface. Applying the conservation of energy principle to each region and across the interface produced three energy equations.

Non-dimensionalization of each equation gave rise to the ratios of thermal diffusivity and thermal conductivity. Considering these parameters unity the integral technique of reducing a partial differential equation to a system of ordinary differential equations was employed. Multiplication of each energy equation by a weighting function in the space variable and then integrating with respect to this space variable

enabled the combination of the three energy equations into one equation representing the entire slab.

The weighting and temperature approximation functions used in applying the integral method (i.e. $\cos n\pi\bar{x}$ and the Fourier cosine series, respectively) were so chosen as to give valid temperatures throughout the slab. These functions are also orthogonal which reduced computations immensely. The fact that the chosen functions do not represent the slope of the temperature validly for all \bar{x} within the slab is not critical since the integrated equation contains no derivatives of temperature with respect to \bar{x} and leads to the so-called weak solution of the original energy equation. It should be noted here that the temperatures obtained by this method can not be differentiated to yield local heat flux values.

The resulting $N+1$ ordinary differential equations along with an additional equation obtained from the condition of constant temperature at the vaporization interface were integrated by a multistep numerical integration routine employing Hamming's modified predictor-corrector technique. Computer solutions employing three, five and seven coefficients in the temperature approximation were generated. While not modeling any particular substances, the temperature profiles and interface velocities obtained appear to be physically realistic. The vaporization process is shown to prevent the temperature of the solid from attaining values which would cause significant pyrolysis.

Conclusions

The following conclusions and observations evolved from this study:

1. The complex analysis of the heating of a saturated porous material

can be divided into two areas of investigation, the vaporization of the liquid initially present, which was the object of this study and the pyrolysis of the dry solid material remaining after vaporization.

2. The discontinuity of the derivative of temperature with respect to time and the spacial coordinate at the interface represents the main difficulty in solving this problem. A transformation of coordinates is possible but results in singularities at the front and back surfaces. Thus in order to initialize the vaporization process a finite distance into the slab must be approximated. The division of the slab into regions, with the application of the integral method to reduce and combine the resulting energy equations into one, thereby eliminating the discontinuity from the problem, results in a weak solution of the problem. This approach appears to be the most practical.

3. Two non-dimensional parameters, the ratios of thermal diffusivity and thermal conductivity, appear in the analysis of the problem. The incorporation of these parameters in the resultant energy equation must be resolved in future studies if known liquids and solids are to be considered in various degrees of combination.

4. The effects of the escaping vapor, neglected in this study, might be included in future studies depending on the magnitude and type of heat flux applied at the exposed surface.

5. The vaporization problem solved in this study, while pertaining to no known substances, appears physically valid. By resolving the thermal diffusivity and thermal conductivity parameters, this study can be combined with previous pyrolysis studies to yield solutions of the heating of a saturated slab from the initial application of a heat flux to the surface ignition of the solid substance.

BIBLIOGRAPHY

1. Alvares, N. J. "Measurements of the Temperature of the Thermally Irradiated Surface of Alpha-Cellulose." USNRDL TR-735, March, 1964.
2. Alvares, N. J., and S. B. Martin. "Mechanism of Ignition of Thermally Irradiated Cellulose." Presented at the XIII International Symposium on Combustion, the Combustion Institute, August 23-29, 1970, Salt Lake City.
3. Bamford, C. H., J. Crank, and D. H. Malan. "The Combustion of Wood, Part I." Proc. of Camb. Phil. Soc., Vol. 42, 1946, p. 166.
4. Belotserkovskii, O. M. and P. I. Chushkin. "A Numerical Method of Integral Relations." (tr.) USSR Comp. Math. and Math. Phy., Vol. 5, 1963, p. 823.
5. Bird, Byron R., Warren E. Stewart, and Edwin N. Lightfoot. Transport Phenomena. John Wiley and Sons, 1960.
6. Bradley, H. H., Jr. "Theory of Ignition of a Reactive Solid by Constant Energy Flux." Combustion Science and Technology, Vol. 2, 1970, pp. 11-20.
7. Carnahan, Brice, H. A. Luther, and James O. Wilkes. Applied Numerical Methods. John Wiley and Sons, 1969.
8. Carslaw, H. S. and J. C. Jenger. Conduction of Heat in Solids. Oxford Press, Second Edition, 1959.
9. Goodman, Theodore R. "Application of Integral Methods to Transient Nonlinear Heat Transfer." Advances in Heat Transfer, ed. Thomas F. Irvine, Jr. and James P. Hartnett, Vol. 1, p. 51, Academic Press, 1964.
10. Goodman, Theodore R., and John H. Shea. "The Melting of Finite Slabs." Trans. ASME, J. of Applied Mech., Vol. 27, 1960, p. 16.
11. Heitz, W. L., and J. W. Westwater. "Extension of the Numerical Method for Melting and Freezing Problem." Int. J. Heat and Mass Transfer, Vol. 13, 1970, pp. 1371-1375.

12. Lazaridis, Anastas. "A Numerical Solution of the Multidimensional Solidification (or Melting) Problem." Int. J. Heat and Mass Transfer, Vol. 13, 1970, pp. 1459-1477.
13. Longwell, P. A. "A Graphical Method for Solution of Freezing Problems." A. I. Ch. E. Jour., Vol. 4, No. 1, March 1958, p. 53.
14. Martin, Stanley. "Diffusion - Controlled Ignition of Cellulosic Materials by Intense Radiation Energy." Tenth Symposium (International) on Combustion, The Combustion Institute, 1966, p. 285.
15. Muehlbauer, John C., and J. Edward Sunderland. "Heat Conduction With Freezing or Melting." Applied Mechanics Reviews, Vol. 18, No. 12, December 1965, p. 951.
16. Murray, William D., and Fred Landis. "Numerical and Machine Solutions of Transient Heat-Conduction Problems Involving Melting or Freezing, Part I - Method of Analysis and Sample Solutions." Trans. ASME, Vol. 81, 1959, p. 106.
17. Myers, Glen E. Analytical Methods in Conduction Heat Transfer. McGraw-Hill, 1971.
18. Özisik, Necati M. Boundary Value Problems of Heat Conduction. International Textbook Company, 1968.
19. Parker, Jerald D. James H. Boggs, and Edward F. Blick. Introduction to Fluid Mechanics and Heat Transfer. Addison-Wesley, 1969.
20. Ralston, Anthony. "Numerical Integration Methods for the Solution of Ordinary Differential Equations." Mathematical Methods for Digital Computers, Volume I, ed. Anthony Ralston and Herbert S. Wilf, John Wiley and Sons, 1960.
21. Rittmann, Jerrold E. "A Computer Study of the Pyrolysis of Porous Solids." (Unpub. Ph. D. Thesis, Oklahoma State University, 1970).
22. Rose, J. Dynamic Physical Chemistry. John Wiley and Sons, 1961.
23. Stratta, J. John, and William L. Livingston, SFPE. "Ablative Fluids in the Fire Environment." Fire Technology, Vol. 5, No. 3, August 1969, p. 181.
24. International Business Machines Corporation. System/360 Scientific Subroutine Package Version III Programmer's Manual. Fifth Edition (August 1970).

25. Weatherfore, W. D., Jr. and D. M. Sheppard. "Basic Studies of the Mechanism of Ignition of Cellulosic Materials." Tenth Symposium (International) on Combustion, The Combustion Institute, 1967, p. 897.

APPENDIX A

EFFECTS OF VAPOR EFFLUX

The effects on the dry region caused by the escaping vapor involves consideration of flow through a porous media, free convection, and forced convection. Ignoring free convection the porosity of the solid and the velocity of the vapor must be known to correctly evaluate the hindrance or contribution of the vapor efflux to the heating of the slab. Since the porosity of the solid and the velocity of the vapor are not known, term V of equation (2.7) will be used. This term expresses the net rate of thermal energy convected per unit volume by the vapor as it escapes through the pores of the dry solid

$$\frac{\partial}{\partial x} \rho_v v_v \left[u_v + \frac{1}{\rho_v} P_v \right] = \frac{\partial}{\partial x} \rho_v v_v h_v \quad (A.1)$$

At the interface the mass-flow rate of vapor per unit area is equal to the mass flow rate of liquid per unit area. Thus assuming this mass flow rate is constant through the dry solid

$$\rho_v v_v = \rho_l v_l \quad (A.2)$$

Substituting (A.2) into (A.1) yields

$$\frac{\partial}{\partial x} \rho_l v_l h_v \quad (A.3)$$

Considering the velocity of the liquid equal to the interface velocity (A.3) is then

$$\frac{\partial}{\partial x} \rho_l \frac{d\ell}{dt} h_v$$

or, since the mass flow rate is assumed constant

$$\rho_l \frac{dl}{dt} \frac{\partial}{\partial x} h_v \quad (\text{A.4})$$

Enthalpy is a function of temperature alone, at constant pressure, thus

$$\rho_l \frac{dl}{dt} \frac{\partial}{\partial x} \int (C_{P_v} dt) = \rho_l \frac{dl}{dt} C_{P_v} \frac{dT}{dx} \quad (\text{A.5})$$

From the non-dimensionalization of variables

$$x = \bar{x}L$$

$$l = \bar{l}L$$

$$\frac{dl}{dt} = \frac{\alpha_w}{L} \frac{d\bar{l}}{d\bar{t}_w}$$

$$\frac{dT}{dx} = \frac{1}{L} \frac{q_o L}{K_w} [\bar{T}_o - \bar{T}_v]$$

where \bar{T}_o is the non-dimensional temperature at the front surface. Substituting these values into (A.5) yields

$$\rho_l \frac{d\bar{l}}{d\bar{t}_w} C_{P_v} \frac{dT}{dx} = \rho_l C_{P_v} \frac{K_w}{C_w \rho_w L} \frac{d\bar{l}}{d\bar{t}_w} \frac{1}{L} [\bar{T}_o - \bar{T}_v] \frac{q_o L}{K_w} \quad (\text{A.6})$$

Picking

$$\frac{q_o L}{K_w} = 300^\circ \text{K}$$

and considering saturated water, saturated steam, and white fir as the porous solid yields

$$\rho_l = 60.053 \text{ lb}_m/\text{ft}^3$$

$$C_{P_v} = .4764 \text{ Btu}/\text{lb}_m \text{ } ^\circ\text{F}$$

$$K_w = .1286 \text{ Btu ft}/\text{hr ft}^2 \text{ } ^\circ\text{F}$$

$$\rho_w C_w = 26.406 \text{ Btu}/\text{ft}^3 \text{ } ^\circ\text{F}$$

$$L = 1 \text{ cm} = .3937 \text{ ft}$$

Choosing the interface at a point midway into the slab for the seven coefficient computational run

$$\frac{d\bar{l}}{d\bar{t}_W} = .96949$$

$$\bar{T}_O - \bar{T}_V = .37407$$

Therefore,

$$\begin{aligned} [\bar{T}_O - \bar{T}_V] \frac{q_o L}{K_W} &= [.37407] 300^\circ \text{K} \\ &= 112.212 \text{ K}^\circ \\ &= 1.8 [112.212] \text{ R}^\circ \\ &= 201.98 \text{ F}^\circ \end{aligned}$$

$$\frac{\rho_l C_{P_V} K_W}{\rho_W C_{W_I} L^2} = \frac{(60.053)(.4764)(.1286)}{(26.406)(.3937)^2} \frac{\text{Btu}}{\text{hr ft}^3 \text{ OF}} = .899 \frac{\text{Btu}}{\text{hr ft}^3 \text{ OF}}$$

Thus

$$\rho_l \frac{dl}{dt} C_{P_V} \frac{dT}{dx} = (.899)(.96949)(201.98) \frac{\text{Btu}}{\text{hr ft}^3} = 176.04 \frac{\text{Btu}}{\text{hr ft}^3}$$

On a unit volume basis the vapor is considered to occupy 20% of the volume, the convective term then yields

$$.2 \text{ ft}^3 (176.04) \frac{\text{Btu}}{\text{hr ft}^3} = 35.21 \frac{\text{Btu}}{\text{hr}} \quad (\text{A.7})$$

The vapor negotiates a positive temperature gradient, therefore this thermal energy can be considered convected away from the solid. The heat flux at the front surface for this example is

$$q_o = \frac{(.1286)(1.8)(300)}{.3937} \frac{\text{Btu}}{\text{hr ft}^2} = 176.39 \frac{\text{Btu}}{\text{hr ft}^2}$$

On a unit volume basis multiplying by the area and dividing by the volume

$$\frac{A}{V} q_o = \frac{176.39}{L} \frac{\text{Btu}}{\text{hr ft}^3} = 448.032 \frac{\text{Btu}}{\text{hr ft}^3}$$

Multiplying by the percent of volume occupied by the solid yields

$$A q_o = .8 \text{ ft}^3 (448.032) \frac{\text{Btu}}{\text{hr ft}^3} = 358.43 \frac{\text{Btu}}{\text{hr}} \quad (\text{A.8})$$

The ratio of the thermal energy convected by the vapor to the heat flux available to the solid is on the order of

$$\frac{35.21}{358.43} = .0982$$

APPENDIX B

NON-DIMENSIONALIZATION OF EQUATIONS

AND BOUNDARY CONDITIONS

Division of x and $l(t)$ by the characteristic length L yields

$$\bar{x} = \frac{x}{L}$$

$$\bar{l}(t) = \frac{l(t)}{L}$$

The non-dimensional temperature \bar{T} and time \bar{t} are chosen as

$$\bar{T} = \frac{T}{T_z}$$

$$\bar{t} = \frac{t}{t_z}$$

where

$$T = T_A - T_R$$

Substituting these terms into equation (2.6)

$$\rho_W C_W \frac{T_z}{t_z} \frac{\partial \bar{T}(\bar{x}, \bar{t}_W)}{\partial \bar{t}_W} = K_W \frac{T_z}{L^2} \frac{\partial^2 \bar{T}(\bar{x}, \bar{t}_W)}{\partial \bar{x}^2} \quad 11$$

rearranging

$$\frac{\partial \bar{T}(\bar{x}, \bar{t}_W)}{\partial \bar{t}_W} = \left(\frac{K_W}{\rho_W C_W} \right) \left(\frac{t_z}{L^2} \right) \frac{\partial^2 \bar{T}(\bar{x}, \bar{t}_W)}{\partial \bar{x}^2}$$

¹¹ The subscripts W and D refer to the wetted and dry regions, respectively.

The thermal diffusivity is defined as

$$\frac{K_W}{C_W \rho_W} = \alpha_W$$

Now t_z can be defined as

$$t_z = \frac{L^2}{\alpha_W}$$

Here t_z is not a time constant as such but is a "significant time" or time scale of the problem. By rearranging, t_z can be shown to represent the product of the thermal capacitance and the internal thermal resistance (17).

$$t_z = \frac{L^2}{\alpha_W} = \frac{\rho_W C_W L^2}{K_W} = \rho_W C_W L A \frac{L}{A K_W} = \rho_W V C_W \left(\frac{L}{K_W A} \right)$$

Therefore \bar{t}_W becomes the Fourier number

$$\bar{t}_W = \frac{t \alpha_W}{L^2}$$

Equation (2.6) is then

$$\frac{\partial \bar{T}(\bar{x}, \bar{t}_W)}{\partial \bar{t}_W} = \frac{\partial^2 \bar{T}(\bar{x}, \bar{t}_W)}{\partial \bar{x}^2} \quad (\text{B.1})$$

In a similar manner, equation (2.8) can be non-dimensionalized, letting

$$\begin{aligned} \bar{\rho}_D(\bar{x}, \bar{t}_D) &= \frac{\rho_D(x, t)}{\rho_D(x, 0)} \\ \left(\rho_D(x, 0) \frac{T_z}{t_z} \right) \bar{\rho}_D(\bar{x}, \bar{t}_D) C_D \frac{\partial \bar{T}(\bar{x}, \bar{t}_D)}{\partial \bar{t}_D} + \left(\rho_D(x, 0) \frac{T_z}{t_z} \right) C_D \bar{T}(\bar{x}, \bar{t}_D) \frac{\partial \bar{\rho}_D(\bar{x}, \bar{t}_D)}{\partial \bar{t}_D} \\ &= \left(\frac{T_z}{L^2} \right) K_D \frac{\partial^2 \bar{T}(\bar{x}, \bar{t}_D)}{\partial \bar{x}^2} \end{aligned}$$

rearranging

$$\frac{\partial \bar{T}(\bar{x}, \bar{t}_D)}{\partial \bar{t}_D} + \frac{\bar{T}(\bar{x}, \bar{t}_D)}{\bar{\rho}_D(\bar{x}, \bar{t}_D)} \frac{\partial \bar{\rho}_D(\bar{x}, \bar{t}_D)}{\partial \bar{t}_D} = \left(\frac{K_D}{C_D \rho_D} \frac{t_z}{L^2} \right) \frac{\partial^2 \bar{T}(\bar{x}, \bar{t}_D)}{\partial \bar{x}^2}$$

Again defining thermal diffusivity

$$\frac{K_D}{C_D \rho_D} = \alpha_D$$

Choosing

$$t_z = \frac{L^2}{\alpha_D}$$

yields the Fourier number

$$\bar{t}_D = \frac{t \alpha_D}{L^2}$$

Equation (2.8) thus becomes

$$\frac{\partial \bar{T}(\bar{x}, \bar{t}_D)}{\partial \bar{t}_D} + \frac{\bar{T}(\bar{x}, \bar{t}_D)}{\bar{\rho}_D(\bar{x}, \bar{t}_D)} \frac{\partial \bar{\rho}_D(\bar{x}, \bar{t}_D)}{\partial \bar{t}_D} = \frac{\partial^2 \bar{T}(\bar{x}, \bar{t}_D)}{\partial \bar{x}^2} \quad (\text{B.2})$$

The energy equation at the liquid-vapor interface (2.9) can be written

$$\rho_l h_{fg} \left(\frac{L}{t_z} \right) \frac{d\bar{\ell}(\bar{t})}{d\bar{t}} = K_W \left(\frac{T_z}{L} \right) \frac{\partial \bar{T}(\bar{x}, \bar{t})}{\partial \bar{x}} \Big|_{\bar{x}^-} - K_D \left(\frac{T_z}{L} \right) \frac{\partial \bar{T}(\bar{x}, \bar{t})}{\partial \bar{x}} \Big|_{\bar{x}^+}$$

dividing by K_W and rearranging

$$\left(\frac{h_{fg} L^2 \rho_l}{t_z T_z K_W} \right) \frac{d\bar{\ell}(\bar{t})}{d\bar{t}} = \frac{\partial \bar{T}(\bar{x}, \bar{t})}{\partial \bar{x}} \Big|_{\bar{x}^-} - \left(\frac{K_D}{K_W} \right) \frac{\partial \bar{T}(\bar{x}, \bar{t})}{\partial \bar{x}} \Big|_{\bar{x}^+} \quad (\text{B.3})$$

Considering the boundary condition at the front surface ($x = L$)

$$q_o = K_W \frac{\partial T(x, t)}{\partial x} \Big|_{x=L} = K_W \left(\frac{T_z}{L} \right) \frac{\partial \bar{T}(\bar{x}, \bar{t})}{\partial \bar{x}} \Big|_{\bar{x}=1} = \text{constant}$$

or

$$\frac{\partial \bar{T}(\bar{x}, \bar{t})}{\partial \bar{x}} \Big|_{\bar{x}=1} = \left(\frac{q_o L}{K_W} \right) \frac{1}{T_z}$$

Choosing

$$T_z = \frac{q_o L}{K_W}$$

$$\left. \frac{\partial \bar{T}(\bar{x}, \bar{t})}{\partial \bar{x}} \right|_{\bar{x}=1} = 1$$

and

$$\bar{T}(\bar{x}, \bar{t}) = \frac{T}{q_o L/K_W} = \frac{T_A - T_R}{q_o L/K_W} \quad (\text{B.4})$$

with

$$\bar{t}_W = \frac{L^2}{\alpha_W}$$

then equation (B.3) becomes

$$\left[\frac{h_{fg} \rho_l \alpha_W}{q_o L} \right] \frac{d\bar{l}(\bar{t}_W)}{d\bar{t}_W} = \frac{\partial \bar{T}(\bar{x}, \bar{t}_W)}{\partial \bar{x}} \Big|_{\bar{l}^-} - \left(\frac{K_D}{K_W} \right) \frac{\partial \bar{T}(\bar{x}, \bar{t}_W)}{\partial \bar{x}} \Big|_{\bar{l}^+}$$

defining \bar{H} as a non-dimensional parameter,

$$\bar{H} = \frac{h_{fg} \rho_l \alpha_W}{q_o L}$$

yields

$$\bar{H} \frac{d\bar{l}(\bar{t}_W)}{d\bar{t}_W} = \frac{\partial \bar{T}(\bar{x}, \bar{t}_W)}{\partial \bar{x}} \Big|_{\bar{l}^-} - \left(\frac{K_D}{K_W} \right) \frac{\partial \bar{T}(\bar{x}, \bar{t}_W)}{\partial \bar{x}} \Big|_{\bar{l}^+} \quad (\text{B.5})$$

From the boundary condition at the interface (2.26) and the non-dimensional temperature (B.4)

$$\bar{T}(\bar{l}, \bar{t}) = \bar{T}_V = \text{constant}$$

$$\bar{T}(\bar{l}, \bar{t}_W) = \frac{T_A - T_R}{T_z} = \frac{T_V - T_R}{q_o L/K_W}$$

or

$$\bar{T}(\bar{l}, \bar{t}_D) = \frac{T_A - T_R}{T_z} = \frac{T_V - T_R}{q_o L/K_D}$$

where

$$\frac{q_o L}{K_D} \bar{T}(\bar{l}, \bar{t}_D) = \frac{q_o L}{K_W} (\bar{l}, \bar{t}_W)$$

$$\bar{T}(\bar{l}, \bar{t}_D) = \frac{K_D}{K_W} \bar{T}(\bar{l}, \bar{t}_W)$$

Thus

$$\bar{T}(\bar{x}, \bar{t}_D) = \frac{K_D}{K_W} \bar{T}(\bar{x}, \bar{t}_W) \quad (\text{B.6})$$

Two Fourier numbers are created by the non-dimensionalization of the energy equations. In order to combine the energy equations properly only one dimensional time can exist. The following relationship is therefore apparent:

$$t = \bar{t}$$

from

$$\bar{t} = \frac{t\alpha}{L^2}$$

$$\bar{t}_D \frac{L^2}{\alpha_D} = \bar{t}_W \frac{L^2}{\alpha_W}$$

$$\bar{t}_D = \frac{\alpha_D}{\alpha_W} \bar{t}_W \quad (\text{B.7})$$

Adopting $\bar{T}(\bar{x}, \bar{t}_W)$ and \bar{t}_W as standards, equations (B.1) and (B.5) remain unchanged but equation (B.2) is transformed to

$$\frac{K_D}{K_W} \frac{\partial \bar{T}(\bar{x}, \bar{t}_W)}{\partial \bar{t}_W} + \frac{K_D}{K_W} \frac{\bar{T}(\bar{x}, \bar{t}_W)}{\bar{\rho}_D(\bar{x}, \bar{t}_W)} \frac{\partial \bar{\rho}_D(\bar{x}, \bar{t}_W)}{\partial \bar{t}_W} = \frac{K_D}{K_W} \frac{\partial^2 \bar{T}(\bar{x}, \bar{t}_W)}{\partial \bar{x}^2}$$

$$\frac{\partial \bar{T}(\bar{x}, \bar{t}_W)}{\partial \bar{t}_W} + \frac{\bar{T}(\bar{x}, \bar{t}_W)}{\bar{\rho}_D(\bar{x}, \bar{t}_W)} \frac{\partial \bar{\rho}_D(\bar{x}, \bar{t}_W)}{\partial \bar{t}_W} = \frac{\alpha_D}{\alpha_W} \frac{\partial^2 \bar{T}(\bar{x}, \bar{t}_W)}{\partial \bar{x}^2} \quad (\text{B.8})$$

Defining parameters \bar{A} and \bar{K} as

$$\bar{A} = \frac{\alpha_D}{\alpha_W}$$

$$\bar{K} = \frac{K_D}{K_W}$$

equations (2.17) through (2.19) are obtained.

APPENDIX C

INTEGRATION OF EQUATION (3.1)

Each term of equation (3.1) can be integrated as shown

$$\int_0^{\bar{l}(\bar{t}_W)} Q(\bar{x}) \frac{\partial \bar{T}(\bar{x}, \bar{t}_W)}{\partial \bar{t}_W} d\bar{x} = \int_0^{\bar{l}(\bar{t}_W)} Q(\bar{x}) \frac{\partial^2 \bar{T}(\bar{x}, \bar{t}_W)}{\partial \bar{x}^2} d\bar{x}$$

I II

Applying Leibnitz's formula to term I

$$\begin{aligned} \frac{d}{d\bar{t}_W} \int_0^{\bar{l}(\bar{t}_W)} Q(\bar{x}) \bar{T}(\bar{x}, \bar{t}_W) d\bar{x} &= \int_0^{\bar{l}(\bar{t}_W)} Q(\bar{x}) \frac{\partial \bar{T}(\bar{x}, \bar{t}_W)}{\partial \bar{t}_W} d\bar{x} \\ &\quad + Q(\bar{x}) \bar{T}(\bar{x}, \bar{t}_W) \frac{\partial \bar{l}(\bar{t}_W)}{\partial \bar{t}_W} \\ &\quad - Q(\bar{x}) \bar{T}(\bar{x}, \bar{t}_W) \frac{\partial (0)}{\partial \bar{t}_W} \end{aligned}$$

rearranging

$$\begin{aligned} \int_0^{\bar{l}(\bar{t}_W)} Q(\bar{x}) \frac{\partial \bar{T}(\bar{x}, \bar{t}_W)}{\partial \bar{t}_W} d\bar{x} &= \frac{d}{d\bar{t}_W} \int_0^{\bar{l}(\bar{t}_W)} Q(\bar{x}) \bar{T}(\bar{x}, \bar{t}_W) d\bar{x} \\ &\quad - Q(\bar{x}) \bar{T}(\bar{x}, \bar{t}_W) \frac{\partial \bar{l}(\bar{t}_W)}{\partial \bar{t}_W} \end{aligned} \tag{C.1}$$

Integrating term II by parts

$$\int_0^{\bar{l}(\bar{t}_W)} Q(\bar{x}) \frac{\partial^2 \bar{T}(\bar{x}, \bar{t}_W)}{\partial \bar{x}^2} d\bar{x} = Q(\bar{x}) \frac{\partial \bar{T}(\bar{x}, \bar{t}_W)}{\partial \bar{x}} \Big|_0^{\bar{l}(\bar{t}_W)} - \int_0^{\bar{l}(\bar{t}_W)} Q'(\bar{x}) \frac{\partial \bar{T}(\bar{x}, \bar{t}_W)}{\partial \bar{x}} d\bar{x}$$

Integrating once again by parts yields

$$\int_0^{\bar{l}(\bar{t}_W)} Q(\bar{x}) \frac{\partial^2 \bar{T}(\bar{x}, \bar{t}_W)}{\partial \bar{x}^2} d\bar{x} = Q(\bar{x}) \frac{\partial \bar{T}(\bar{x}, \bar{t}_W)}{\partial \bar{x}} \Big|_0^{\bar{l}(\bar{t}_W)} - Q'(\bar{x}) \bar{T}(\bar{x}, \bar{t}_W) \Big|_0^{\bar{l}(\bar{t}_W)} + \int_0^{\bar{l}(\bar{t}_W)} Q''(\bar{x}) \bar{T}(\bar{x}, \bar{t}_W) d\bar{x} \quad (C.2)$$

Substituting (C.1) and (C.2) into equation (3.1) yields equation (3.2).

APPENDIX D

INTEGRATION OF EQUATION (3.3)

Each term of equation (3.3) can be integrated as shown

$$\int_{\bar{l}(\bar{t}_W)}^1 Q(\bar{x}) \frac{\partial \bar{T}(\bar{x}, \bar{t}_W)}{\partial \bar{t}_W} d\bar{x} = \bar{A} \int_{\bar{l}(\bar{t}_W)}^1 Q(\bar{x}) \frac{\partial^2 \bar{T}(\bar{x}, \bar{t}_W)}{\partial \bar{x}^2} d\bar{x}$$

I II

Applying Leibnitz's formula to term I

$$\begin{aligned} \frac{d}{d\bar{t}_W} \int_{\bar{l}(\bar{t}_W)}^1 Q(\bar{x}) \bar{T}(\bar{x}, \bar{t}_W) d\bar{x} &= \int_{\bar{l}(\bar{t}_W)}^1 Q(\bar{x}) \frac{\partial \bar{T}(\bar{x}, \bar{t}_W)}{\partial \bar{t}_W} d\bar{x} \\ &\quad \text{Term I} \\ &\quad + Q(\bar{x}) \bar{T}(\bar{x}, \bar{t}_W) \frac{\partial 1}{\partial \bar{t}_W} \\ &\quad - Q(\bar{x}) \bar{T}(\bar{x}, \bar{t}_W) \frac{\partial \bar{l}(\bar{t}_W)}{\partial \bar{t}_W} \end{aligned}$$

rearranging

$$\begin{aligned} \int_{\bar{l}(\bar{t}_W)}^1 Q(\bar{x}) \frac{\partial \bar{T}(\bar{x}, \bar{t}_W)}{\partial \bar{t}_W} d\bar{x} &= \frac{d}{d\bar{t}_W} \int_{\bar{l}(\bar{t}_W)}^1 Q(\bar{x}) \bar{T}(\bar{x}, \bar{t}_W) d\bar{x} \\ &\quad + Q(\bar{x}) \bar{T}(\bar{x}, \bar{t}_W) \frac{\partial \bar{l}(\bar{t}_W)}{\partial \bar{t}_W} \end{aligned} \tag{D.1}$$

Integrating term II by parts

$$\begin{aligned} \bar{A} \int_{\bar{l}(\bar{t}_W)}^1 Q(\bar{x}) \frac{\partial^2 \bar{T}(\bar{x}, \bar{t}_W)}{\partial \bar{x}^2} d\bar{x} &= \bar{A} Q(\bar{x}) \frac{\partial \bar{T}(\bar{x}, \bar{t}_W)}{\partial \bar{x}} \Big|_{\bar{l}(\bar{t}_W)}^1 \\ &- \bar{A} \int_{\bar{l}(\bar{t}_W)}^1 Q'(\bar{x}) \frac{\partial \bar{T}(\bar{x}, \bar{t}_W)}{\partial \bar{x}} d\bar{x} \end{aligned}$$

Integrating once again by parts yields

$$\begin{aligned} \bar{A} \int_{\bar{l}(\bar{t}_W)}^1 Q(\bar{x}) \frac{\partial^2 \bar{T}(\bar{x}, \bar{t}_W)}{\partial \bar{x}^2} d\bar{x} &= \bar{A} Q(\bar{x}) \frac{\partial \bar{T}(\bar{x}, \bar{t}_W)}{\partial \bar{x}} \Big|_{\bar{l}(\bar{t}_W)}^1 \\ &- \bar{A} Q'(\bar{x}) \bar{T}(\bar{x}, \bar{t}_W) \Big|_{\bar{l}(\bar{t}_W)}^1 \\ &+ \bar{A} \int_{\bar{l}(\bar{t}_W)}^1 Q''(\bar{x}) \bar{T}(\bar{x}, \bar{t}_W) d\bar{x} \end{aligned}$$

Substituting (D.1) and (D.2) into equation (3.3) yields equation (3.4).

APPENDIX E

DERIVATION OF EQUATIONS (3.10) AND (3.11)

Substituting equations (3.8) and (3.9) into equation (3.7) yields

$$\begin{aligned}
 & \frac{d}{d\bar{t}_W} \int_0^1 \cos(m\pi \bar{x}) \sum_{n=0}^N A_n(\bar{t}_W) \cos(n\pi \bar{x}) d\bar{x} = \\
 & \quad \text{I} \\
 & \quad \cos(m\pi \bar{x}) \Big|_{\bar{x}=\bar{\ell}} \bar{H} \frac{d\bar{\ell}(\bar{t}_W)}{d\bar{t}_W} + \cos(m\pi) \quad \text{II} \quad \text{III} \\
 & \quad - (m\pi) \sin(m\pi \bar{x}) \sum_{n=0}^N A_n(\bar{t}_W) \cos(n\pi \bar{x}) \Big|_{\bar{x}=0} \quad \text{IV} \\
 & \quad + (m\pi) \sin(m\pi \bar{x}) \sum_{n=0}^N A_n(\bar{t}_W) \cos(n\pi \bar{x}) \Big|_{\bar{x}=1} \quad \text{V} \\
 & \quad - \int_0^1 (m\pi)^2 \cos(m\pi \bar{x}) \sum_{n=0}^N A_n(\bar{t}_W) \cos(n\pi \bar{x}) d\bar{x} \quad \text{VI} \quad \text{(E.1)}
 \end{aligned}$$

For $\bar{x} = 0$

$$\sin(m\pi \bar{x}) = \sin(0) = 0.$$

For $\bar{x} = 1$, $\sin(m\pi \bar{x})$ reduces to $\sin(m\pi)$ which is zero for

$m = 0, 1, 2, \dots, M$, therefore terms IV and V are zero. Since the cosine is

an orthogonal function to itself on the interval $[0,1]$, terms I and VI exist for $m = n$ only and are zero for all $m \neq n$. Equation (E.1) reduces to

$$\int_0^1 \cos^2 (n\pi \bar{x}) \frac{dA_n(\bar{t}_W)}{d\bar{t}_W} d\bar{x} = \cos (n\pi \bar{l}) \bar{H} \frac{d\bar{l}(\bar{t}_W)}{d\bar{t}} + \cos (n\pi) - \int_0^1 (n\pi)^2 \cos^2 (n\pi \bar{x}) A_n(\bar{t}_W) d\bar{x}$$

rearranging

$$\frac{dA_n(\bar{t}_W)}{d\bar{t}_W} \int_0^1 \cos^2 (n\pi \bar{x}) d\bar{x} = \cos (n\pi \bar{l}) \bar{H} \frac{d\bar{l}(\bar{t}_W)}{d\bar{t}_W} + \cos (n\pi) - (n\pi)^2 A_n(\bar{t}_W) \int_0^1 \cos^2 (n\pi \bar{x}) d\bar{x} \quad (E.2)$$

for $n \neq 0$

$$\int_0^1 \cos^2 (n\pi \bar{x}) d\bar{x} = \left[\frac{1}{2} \bar{x} + \frac{1}{4\pi n} \sin (2n\pi \bar{x}) \right]_0^1 = \frac{1}{2} \bar{x} \Big|_0^1 = \frac{1}{2}$$

Equation (E.2) consequently becomes

$$\frac{dA_n(\bar{t}_W)}{d\bar{t}_W} = 2 \cos (n\pi \bar{l}) \bar{H} \frac{d\bar{l}(\bar{t}_W)}{d\bar{t}_W} + 2 \cos (n\pi) - (n\pi)^2 A_n(\bar{t}_W)$$

for $n = 0$

$$\int_0^1 \cos^2 (0) \pi \bar{x} d\bar{x} = \int_0^1 d\bar{x} = 1$$

Therefore

$$\frac{dA_o(\bar{t}_W)}{d\bar{t}_W} = \bar{H} \frac{d\bar{l}(\bar{t}_W)}{d\bar{t}_W} + 1$$

APPENDIX F

DERIVATION OF EQUATION (3.13)

Expanding the (N+1) equations represented by equations (3.10)

and (3.11)

$$(0) \quad \dot{A}_0 + 0 + \dots - \bar{H} \dot{\bar{l}} = 1^{13}$$

$$(1) \quad 0 + \dot{A}_1 + \dots - 2\bar{H} \dot{\bar{l}} \cos(\pi \bar{l}) = 2 \cos \pi - \pi^2 A_1$$

$$(2) \quad 0 + 0 + A_2 + \dots - 2\bar{H} \dot{\bar{l}} \cos(2\pi \bar{l}) = 2 \cos(2\pi) - (2\pi)^2 A_2$$

$$(N) \quad 0 + 0 + \dots + \dot{A}_N - 2\bar{H} \dot{\bar{l}} \cos(N\pi \bar{l}) = 2 \cos(N\pi) - (N\pi)^2 A_N$$

Expanding equation (3.12) also

$$\dot{A}_0 + \dot{A}_1 \cos(\pi \bar{l}) + \dot{A}_2 \cos(2\pi \bar{l}) + \dots + \dot{A}_N \cos(N\pi \bar{l})$$

$$- \dot{\bar{l}} \sum_{j=1}^N (j\pi) A_j \sin(j\pi \bar{l}) = 0$$

Multiplying each (n) equation by $\cos(n\pi \bar{l})$ and subtracting in turn each (n) equation from equation (3.12) produces

¹³The dot used here indicates differentiation with respect to time (e.g. $\dot{A}_0 = dA_0(\bar{t}_W)/d\bar{t}_W$).

$$\dot{\bar{l}} \left\{ \bar{H} \left[1 + 2 \sum_{j=1}^N \cos^2 (j\pi \bar{l}) \right] - \sum_{j=1}^N (j\pi) A_j \sin (j\pi \bar{l}) \right\} =$$

$$- \left\{ 1 + 2 \sum_{j=1}^N \left[\cos (j\pi) \cos (j\pi \bar{l}) \right] \right\} + \sum_{j=1}^N (j\pi)^2 A_j \cos (j\pi \bar{l})$$

Solving for $\dot{\bar{l}}$ yields equation (3.13)

$$\dot{\bar{l}} = - \frac{\left\{ 1 + 2 \sum_{j=1}^N \left[\cos (j\pi) \cos (j\pi \bar{l}) \right] \right\} - \sum_{j=1}^N (j\pi)^2 A_j \cos (j\pi \bar{l})}{\bar{H} \left\{ 1 + 2 \sum_{j=1}^N \cos^2 (j\pi \bar{l}) \right\} - \sum_{j=1}^N (j\pi) A_j \sin (j\pi \bar{l})}$$

APPENDIX G

INTEGRATION OF EQUATION (3.14)

Rearranging equation (3.14)

$$\frac{d}{d\bar{t}_W} A_n(\bar{t}_W) + (n\pi)^2 A_n(\bar{t}_W) = 2 \cos(n\pi)$$

This is a first order ordinary differential equation of which the integration factor is

$$\mu = \exp(n\pi)^2 \bar{t}_W$$

Thus

$$\frac{d}{d\bar{t}_W} \left(A_n \exp(n\pi)^2 \bar{t}_W \right) = \left(2 \cos(n\pi) \right) \exp(n\pi)^2 \bar{t}_W$$

or integrating

$$A_n(\bar{t}_W) \exp(n\pi)^2 \bar{t}_W = \frac{2 \cos(n\pi)}{(n\pi)^2} \exp(n\pi)^2 \bar{t}_W + c$$

Multiplying by

$$\exp[-(n\pi)^2 \bar{t}_W]$$

$$A_n(\bar{t}_W) = \frac{2(-1)^n}{(n\pi)^2} + c \exp[-(n\pi)^2 \bar{t}_W] \quad (G.1)$$

for $\bar{t}_W = 0$

$$A_n(\bar{t}_W) = 0 \quad (n > 0)$$

Therefore from (G.1)

$$0 = \frac{2(-1)^n}{(n\pi)^2} + c \exp[-(n\pi)^2 (0)]$$

or

$$c = - \frac{2(-1)^n}{(n\pi)^2}$$

and finally

$$A_n(\bar{t}_W) = \frac{2(-1)^n}{(n\pi)^2} \left\{ \exp \left[- (n\pi)^2 \bar{t}_W \right] - 1 \right\}$$

APPENDIX H

EVALUATION OF PARAMETERS \bar{A} AND \bar{K}

To obtain some idea of the relevance of these non-dimensional parameters, water and white fir are considered in a volumetric ratio of one to four.

The mean specific heats of water and white fir in the temperature range of 32-212° F are approximately

$$C_{H_2O} = 1.004 \text{ Btu/lb}_m \text{ } ^\circ\text{F}$$

$$C_{fir} = .65 \text{ Btu/lb}_m \text{ } ^\circ\text{F}$$

The average densities of these substances within the same temperature range are approximately

$$\rho_{H_2O} = 61.582 \text{ lb}_m/\text{ft}^3$$

$$\rho_{fir} = 27.0 \text{ lb}_m/\text{ft}^3$$

Assuming constant thermal conductivities of

$$K_{H_2O} = .367 \text{ Btu ft/hr ft}^2 \text{ } ^\circ\text{F}$$

$$K_{fir} = .069 \text{ Btu ft/hr ft}^2 \text{ } ^\circ\text{F}$$

On a unit volumetric basis

$$K_w = .8(K_{fir}) + .2(K_{H_2O})$$

$$K_w = .1286 \text{ Btu ft/hr ft}^2 \text{ } ^\circ\text{F}$$

Therefore,

$$\bar{K} = \frac{K_D}{K_W} = \frac{K_{\text{fir}}}{K_W} = .537$$

From Table II

$$\bar{A} = \frac{\alpha_D}{\alpha_W} = \frac{K_D}{K_W} \cdot \frac{\rho_W^C}{\rho_D^C} = \bar{K} \cdot \frac{\rho_W^C}{\rho_D^C}$$

where

$$\begin{aligned} \rho_W^C &= .8(\rho_{\text{FIR}}^C) + .2(\rho_{\text{H}_2\text{O}}^C) \\ &= (14.04 + 12.366) \text{ Btu/ft}^3 \text{ } ^\circ\text{F} \\ &= 26.406 \text{ Btu/ft}^3 \text{ } ^\circ\text{F} \end{aligned}$$

and

$$\rho_D^C = \rho_{\text{fir}}^C = 17.55 \text{ Btu/ft}^3 \text{ } ^\circ\text{F}$$

Therefore,

$$\bar{A} = (.537) \frac{26.406}{17.55} = .808$$

APPENDIX I

COMPUTER LISTING OF ALL PROGRAMS

80/80 LIST

```

000000000111111112222222223333333334444444445555555556666666667777777778
12345678901234567890123456789012345678901234567890123456789012345678901234567890
CARD
0001 C *****MAIN0010
0002 C***          MAIN SECTION          *****MAIN0020
0003 C***          (INITIALIZATION)      *****MAIN0030
0004 C*****MAIN0040
0005 EXTERNAL DERFUN,DEROUT          MAIN0050
0006 DOUBLE PRECISION ETA1(10),ETA2(10),H,DLDT,G,TV,T,ONE,ZERO,CH20, MAIN0060
0007 *          TEND,TMIN,TPRT,PI,EL,DELI          MAIN0070
0008 COMMON/COM1/ETA1,ETA2,H,DLDT,G,TV,T,ONE,ZERO,CH20,TEND,TMIN,TPRT, MAIN0080
0009 *          PI,EL,DELI,          MAIN0090
0010 *          N,MCOUNT,NPRINT,NSTEP,ISTEP,ISTART, MAIN0100
0011 *          NM1,NP1,NP2          MAIN0110
0012 DOUBLE PRECISION TX,Y(36),DERY(36),A(24), MAIN0120
0013 C          MAIN0130
0014 C          THE ABOVE SPECIFICATION CARDS ARE COMMON          MAIN0140
0015 C          TO - 'MAIN' , 'DEROUT' , & 'DERFUN'          MAIN0150
0016 C          THE FOLLOWING SPECIFICATIONS ARE PARTICULAR          MAIN0160
0017 C          TO 'MAIN'          MAIN0170
0018 C          MAIN0180
0019 *          AUX(16,36),PRMT(5),ASUM,BSUM,PINSQ,          MAIN0190
0020 *          HFG,ROW,CP,QO,THERMK,TR,TB,ELL,          MAIN0200
0021 *          DEL,DLMN,ERMX,DCOS,DSIN          MAIN0210
0022 1000 FORMAT(I3)          MAIN0220
0023 1001 FORMAT(D16.8)          MAIN0230
0024 2005 FORMAT('1*****MAIN0240
0025 *****MAIN0250
0026 *****')          MAIN0260
0027 2006 FORMAT(' *****MAIN0270
0028 *****MAIN0280
0029 *****')          MAIN0290
0030 2010 FORMAT(' *****MAIN0300
0031 *** DATA *****MAIN0310
0032 *****')          MAIN0320
0033 2020 FORMAT(' HFG =',E13.6,' POW =',E13.6,' CP =',E13.6,          MAIN0330
0034 * /' TR =',E13.6,' TB =',E13.6,' G =',E13.6,          MAIN0340
0035 * ' QO =',E13.6,' EL =',E13.6,' THERMK =',E13.6          MAIN0350
0036 * ' H =',E13.6,' TV =',E13.6)          MAIN0360
0037 2040 FORMAT(' TEND=',E13.6,' DEL =',E13.6,' DELI=',E13.6,          MAIN0370
0038 * ' ERMX=',E13.6,' DLMN=',E13.6,' TMIN=',E13.6)          MAIN0380
0039 2050 FORMAT(' ',4('ETA1(',I2,')=',E11.5,' '))          MAIN0390
0040 2051 FORMAT(' ',4('ETA2(',I2,')=',E11.5,' '))          MAIN0400
0041 2070 FORMAT(' N = ',I3,5X,'NE = ',I3,5X,'MCOUNT = ',I3,5X,'NPRINT = ',          MAIN0410
0042 * I3,5X,'NSTEP = ',I3,5X,'ISTART = ',I3)          MAIN0420
0043 2222 FORMAT(7I5)          MAIN0430
0044 4000 FORMAT(11H S.S. FOR A)          MAIN0440
0045 4444 FORMAT(4E20.6)          MAIN0450
0046 9000 FORMAT(' ERROR = 11 **** DEL = ',E15.8)          MAIN0460
0047 9001 FORMAT(' ERROR = 12 **** DEL = ',E15.8)          MAIN0470
0048 9002 FORMAT(' ERROR = 13 **** DEL = ',E15.8,5X,'DLMX = ',E15.8,          MAIN0480
0049 * 5X,'DLMN = ',E15.8)          MAIN0490
0050 9010 FORMAT (' ***** ENTIRE TIME INTERVAL EXECUTED TEND = ',          MAIN0500
0051 * D16.6,'***** IHLF = ',I4,'***** PRMT(5) = ',D16.6,'*****')          MAIN0510
0052 9020 FORMAT('0***** NPRINT IS BEYOND CAPABILITY OF PLOTIT *****')          MAIN0520
0053 9030 FORMAT('0 *** ISTART =',I3)          MAIN0530
0054 9701 FORMAT('0',6('A',I2,' =',D14.6,2X))          MAIN0540

```


80/80 LIST

000000001111111122222222333333333333444444445555555566666666777777778
 12345678901234567890123456789012345678901234567890123456789012345678901234567890

```

CARD
0109 10 DO 11 J=1,NP1 MAIN1090
0110 Y(J) = A(J) MAIN1100
0111 11 CONTINUE MAIN1110
0112 Y(NP2) = EL MAIN1120
0113 DERY(NP2) = DLDT MAIN1130
0114 TX = T MAIN1140
0115 CALL DEROUT(TX,Y,DERY,IHLF,NE,PRMT) MAIN1150
0116 IF(PRMT(5).NE.0.000) GO TO 20 MAIN1160
0117 T = T + DELI MAIN1170
0118 A(I) = G * T MAIN1180
0119 DO 12 K=2,NP1 MAIN1190
0120 NN = K-1 MAIN1200
0121 PINSQ = (PI*NN)**2 MAIN1210
0122 A(K) = ((1.000*((-ONE)**NN)*G)/PINSQ)*(ONE-(ONE/DEXP(PINSQ*T))) MAIN1220
0123 12 CONTINUE MAIN1230
0124 GO TO 10 MAIN1240
0125 C***** MAIN1250
0126 C*** START OF INTEGRATION ***MAIN1260
0127 C***** MAIN1270
0128 20 CONTINUE MAIN1280
0129 ISTART = 2 MAIN1290
0130 NCOUNT = 11 MAIN1300
0131 DO 21 I=1,NP1 MAIN1310
0132 Y(I) = A(I) MAIN1320
0133 DERY(I) = ONE/NP2 MAIN1330
0134 21 CONTINUE MAIN1340
0135 DERY(NP2) = ONE/NP2 MAIN1350
0136 Y(NP2) = EL MAIN1360
0137 PRMT(1) = T MAIN1370
0138 PRMT(2) = TEND MAIN1380
0139 PRMT(3) = DEL MAIN1390
0140 PRMT(4) = ERMX MAIN1400
0141 PRMT(5) = ZERO MAIN1410
0142 TPRT = ZERO MAIN1420
0143 GO TO 2 MAIN1430
0144 268 CALL DHPCC(PRMT,Y,DERY,NE,IHLF,DERFUN,DEROUT,AUX) MAIN1440
0145 C***** MAIN1450
0146 C*** RETURN FROM 'DHPCC' ***MAIN1460
0147 C*** IHLF = ' ' ***MAIN1470
0148 C*** 11 - MORE THAN 10 BISECTIONS OF THE INITIAL ***MAIN1480
0149 C*** INTERVAL ARE NECESSARY FOR SATISFACTORY ***MAIN1490
0150 C*** ACCURACY. ***MAIN1500
0151 C*** 12 - INITIAL INCREMENT OF THE INDEPENDENT ***MAIN1510
0152 C*** VARIABLE (DEL) = 0. ***MAIN1520
0153 C*** 13 - SIGN OF (DEL) NOT EQUAL TO THE SIGN OF ***MAIN1530
0154 C*** UPPER BOUND MINUS LOWER BOUND (DLMX-DLMN) ***MAIN1540
0155 C*** ***MAIN1550
0156 C*** OTHERWISE -- THE ENTIRE INTEGRATION INTERVAL MUST HAVE ***MAIN1560
0157 C*** WORKED THROUGH. ***MAIN1570
0158 C***** MAIN1580
0159 269 IF(IHLF.NE.11) GO TO 27 MAIN1590
0160 WRITE(6,9000) DEL MAIN1600
0161 WRITE(6,9702) (I,Y(I),I=1,NE),(I,DERY(I),I=1,NE) MAIN1610
0162 STOP MAIN1620

```


80/80 LIST

```
0000000001111111112222222222333333333344444444445555555555666666666677777777778
12345678901234567890123456789012345678901234567890123456789012345678901234567890

CARD
0163 27 IF(IHLF.NE.12) GO TO 271 MAIN1630
0164 WRITE(6,9001) DEL MAIN1640
0165 STOP MAIN1650
0166 271 IF(IHLF.NE.13) GO TO 28 MAIN1660
0167 WRITE(6,9002) DEL,OLMX,OLMN MAIN1670
0168 STOP MAIN1680
0169 28 WRITE(6,9010) TEND,IHLF,PRMT(5) MAIN1690
0170 STOP MAIN1700
0171 END MAIN1710
0172
0173
```

80/80 LIST

```

00000000011111111122222222333333334444444455555555666666667777777778
1234567890123456789012345678901234567890123456789012345678901234567890
CARD
0001 C ..... DHCG 10
0002 C ..... DHCG 20
0003 C ..... DHCG 30
0004 C SUBROUTINE DHPGC DHCG 40
0005 C DHCG 50
0006 C PURPOSE DHCG 60
0007 C TO SOLVE A SYSTEM OF FIRST ORDER ORDINARY GENERAL DHCG 70
0008 C DIFFERENTIAL EQUATIONS WITH GIVEN INITIAL VALUES. DHCG 80
0009 C DHCG 90
0010 C USAGE DHCG 100
0011 C CALL DHPGC (PRMT,Y,DERY,NDIM,IHLF,FCT,OUTP,AUX) DHCG 110
0012 C PARAMETERS FCT AND OUTP REQUIRE AN EXTERNAL STATEMENT. DHCG 120
0013 C DHCG 130
0014 C DESCRIPTION OF PARAMETERS DHCG 140
0015 C PRMT - DOUBLE PRECISION INPUT AND OUTPUT VECTOR WITH DHCG 150
0016 C DIMENSION GREATER THAN OR EQUAL TO 5, WHICH DHCG 160
0017 C SPECIFIES THE PARAMETERS OF THE INTERVAL AND OF DHCG 170
0018 C ACCURACY AND WHICH SERVES FOR COMMUNICATION BETWEEN DHCG 180
0019 C OUTPUT SUBROUTINE (FURNISHED BY THE USER) AND DHCG 190
0020 C SUBROUTINE DHPGC. EXCEPT PRMT(5) THE COMPONENTS DHCG 200
0021 C ARE NOT DESTROYED BY SUBROUTINE DHPGC AND THEY ARE DHCG 210
0022 C PRMT(1)- LOWER BOUND OF THE INTERVAL (INPUT), DHCG 220
0023 C PRMT(2)- UPPER BOUND OF THE INTERVAL (INPUT), DHCG 230
0024 C PRMT(3)- INITIAL INCREMENT OF THE INDEPENDENT VARIABLE DHCG 240
0025 C (INPUT), DHCG 250
0026 C PRMT(4)- UPPER ERROR BOUND (INPUT). IF ABSOLUTE ERROR IS DHCG 260
0027 C GREATER THAN PRMT(4), INCREMENT GETS HALVED. DHCG 270
0028 C IF INCREMENT IS LESS THAN PRMT(3) AND ABSOLUTE DHCG 280
0029 C ERROR LESS THAN PRMT(4)/50, INCREMENT GETS DOUBLED. DHCG 290
0030 C THE USER MAY CHANGE PRMT(4) BY MEANS OF HIS DHCG 300
0031 C OUTPUT SUBROUTINE. DHCG 310
0032 C PRMT(5)- NO INPUT PARAMETER. SUBROUTINE DHPGC INITIALIZES DHCG 320
0033 C PRMT(5)=0. IF THE USER WANTS TO TERMINATE DHCG 330
0034 C SUBROUTINE DHPGC AT ANY OUTPUT POINT, HE HAS TO DHCG 340
0035 C CHANGE PRMT(5) TO NON-ZERO BY MEANS OF SUBROUTINE DHCG 350
0036 C OUTP. FURTHER COMPONENTS OF VECTOR PRMT ARE DHCG 360
0037 C FEASIBLE IF ITS DIMENSION IS DEFINED GREATER DHCG 370
0038 C THAN 5. HOWEVER SUBROUTINE DHPGC DOES NOT REQUIRE DHCG 380
0039 C AND CHANGE THEM. NEVERTHELESS THEY MAY BE USEFUL DHCG 390
0040 C FOR HANDING RESULT VALUES TO THE MAIN PROGRAM DHCG 400
0041 C (CALLING DHPGC) WHICH ARE OBTAINED BY SPECIAL DHCG 410
0042 C MANIPULATIONS WITH OUTPUT DATA IN SUBROUTINE OUTP. DHCG 420
0043 C Y - DOUBLE PRECISION INPUT VECTOR OF INITIAL VALUES DHCG 430
0044 C (DESTROYED). LATER Y IS THE RESULTING VECTOR OF DHCG 440
0045 C DEPENDENT VARIABLES COMPUTED AT INTERMEDIATE DHCG 450
0046 C POINTS X. DHCG 460
0047 C DERY - DOUBLE PRECISION INPUT VECTOR OF ERROR WEIGHTS DHCG 470
0048 C (DESTROYED). THE SUM OF ITS COMPONENTS MUST BE DHCG 480
0049 C EQUAL TO 1. LATER DERY IS THE VECTOR OF DHCG 490
0050 C DERIVATIVES, WHICH BELONG TO FUNCTION VALUES Y AT DHCG 500
0051 C INTERMEDIATE POINTS X. DHCG 510
0052 C NDIM - AN INPUT VALUE, WHICH SPECIFIES THE NUMBER OF DHCG 520
0053 C EQUATIONS IN THE SYSTEM. DHCG 530
0054 C IHLF - AN OUTPUT VALUE, WHICH SPECIFIES THE NUMBER OF DHCG 540

```

80/80 LIST

```

000000000111111111222222222333333333333334444444445555555556666666667777777778
12345678901234567890123456789012345678901234567890123456789012345678901234567890

CARD
0055 C          BISECTIONS OF THE INITIAL INCREMENT. IF IHLF GETS DHCG 550
0056 C          GREATER THAN 10, SUBROUTINE DHPG RETURNS WITH DHCG 560
0057 C          ERROR MESSAGE IHLF=11 INTO MAIN PROGRAM. DHCG 570
0058 C          ERROR MESSAGE IHLF=12 OR IHLF=13 APPEARS IN CASE DHCG 580
0059 C          PRMT(3)=0 OR IN CASE SIGN(PRMT(3)).NE.SIGN(PRMT(2)-DHCG 590
0060 C          PRMT(1)) RESPECTIVELY. DHCG 600
0061 C          FCT - THE NAME OF AN EXTERNAL SUBROUTINE USED. IT DHCG 610
0062 C          COMPUTES THE RIGHT HAND SIDES DERY OF THE SYSTEM DHCG 620
0063 C          TO GIVEN VALUES OF X AND Y. ITS PARAMETER LIST DHCG 630
0064 C          MUST BE X,Y,DERY. THE SUBROUTINE SHOULD NOT DHCG 640
0065 C          DESTROY X AND Y. DHCG 650
0066 C          OUTP - THE NAME OF AN EXTERNAL OUTPUT SUBROUTINE USED. DHCG 660
0067 C          ITS PARAMETER LIST MUST BE X,Y,DERY,IHLF,NDIM,PRMT. DHCG 670
0068 C          NONE OF THESE PARAMETERS (EXCEPT, IF NECESSARY, DHCG 680
0069 C          PRMT(4),PRMT(5),...) SHOULD BE CHANGED BY DHCG 690
0070 C          SUBROUTINE OUTP. IF PRMT(5) IS CHANGED TO NON-ZERO, DHCG 700
0071 C          SUBROUTINE DHPG IS TERMINATED. DHCG 710
0072 C          AUX - DOUBLE PRECISION AUXILIARY STORAGE ARRAY WITH 16 DHCG 720
0073 C          ROWS AND NDIM COLUMNS. DHCG 730
0074 C          DHCG 740
0075 C          REMARKS DHCG 750
0076 C          THE PROCEDURE TERMINATES AND RETURNS TO CALLING PROGRAM, IF DHCG 760
0077 C          (1) MORE THAN 10 BISECTIONS OF THE INITIAL INCREMENT ARE DHCG 770
0078 C          NECESSARY TO GET SATISFACTORY ACCURACY (ERROR MESSAGE DHCG 780
0079 C          IHLF=11), DHCG 790
0080 C          (2) INITIAL INCREMENT IS EQUAL TO 0 OR HAS WRONG SIGN DHCG 800
0081 C          (ERROR MESSAGES IHLF=12 OR IHLF=13), DHCG 810
0082 C          (3) THE WHOLE INTEGRATION INTERVAL IS WORKED THROUGH, DHCG 820
0083 C          (4) SUBROUTINE OUTP HAS CHANGED PRMT(5) TO NON-ZERO. DHCG 830
0084 C          DHCG 840
0085 C          SUBROUTINES AND FUNCTION SUBPROGRAMS REQUIRED DHCG 850
0086 C          THE EXTERNAL SUBROUTINES FCT(X,Y,DERY) AND DHCG 860
0087 C          OUTP(X,Y,DERY,IHLF,NDIM,PRMT) MUST BE FURNISHED BY THE USER. DHCG 870
0088 C          DHCG 880
0089 C          METHOD DHCG 890
0090 C          EVALUATION IS DONE BY MEANS OF HAMMING'S MODIFIED PREDICTOR- DHCG 900
0091 C          CORRECTOR METHOD. IT IS A FOURTH ORDER METHOD, USING 4 DHCG 910
0092 C          PRECEEDING POINTS FOR COMPUTATION OF A NEW VECTOR Y OF THE DHCG 920
0093 C          DEPENDENT VARIABLES. DHCG 930
0094 C          FOURTH ORDER RUNGE-KUTTA METHOD SUGGESTED BY RALSTON IS DHCG 940
0095 C          USED FOR ADJUSTMENT OF THE INITIAL INCREMENT AND FOR DHCG 950
0096 C          COMPUTATION OF STARTING VALUES. DHCG 960
0097 C          SUBROUTINE DHPG AUTOMATICALLY ADJUSTS THE INCREMENT DURING DHCG 970
0098 C          THE WHOLE COMPUTATION BY HALVING OR DOUBLING. DHCG 980
0099 C          TO GET FULL FLEXIBILITY IN OUTPUT, AN OUTPUT SUBROUTINE DHCG 990
0100 C          MUST BE CODED BY THE USER. DHCG1000
0101 C          FOR REFERENCE, SEE DHCG1010
0102 C          (1) RALSTON/WILF, MATHEMATICAL METHODS FOR DIGITAL DHCG1020
0103 C          COMPUTERS, WILEY, NEW YORK/LONDON, 1960, PP.95-109. DHCG1030
0104 C          (2) RALSTON, RUNGE-KUTTA METHODS WITH MINIMUM ERROR BOUNDS, DHCG1040
0105 C          MTAC, VOL.16, ISS.80 (1962), PP.431-437. DHCG1050
0106 C          DHCG1060
0107 C          ..... DHCG1070
0108 C          DHCG1080

```


80/80 LIST

```

0000000001111111112222222222333333333344444444445555555555666666666677777777778
12345678901234567890123456789012345678901234567890123456789012345678901234567890
CARD
0163          AUX(2,I)=Y(I)                                DHCG1630
0164      14  AUX(9,I)=DERY(I)                              DHCG1640
0165          ISW=3                                         DHCG1650
0166          GOTO 100                                     DHCG1660
0167      C                                             DHCG1670
0168      C      COMPUTATION OF TEST VALUE DELT           DHCG1680
0169      15  DELT=0.00                                     DHCG1690
0170          DO 16 I=1,NDIM                               DHCG1700
0171      16  DELT=DELT+AUX(15,I)*DABS(Y(I)-AUX(4,I))     DHCG1710
0172          DELT=.06666666666666667D0*DELT             DHCG1720
0173          IF(DELT-PRMT(4))19,19,17                    DHCG1730
0174      17  IF(IHLF-10)11,18,18                          DHCG1740
0175      C                                             DHCG1750
0176      C      NO SATISFACTORY ACCURACY AFTER 10 BISECTION. ERROR MESSAGE. DHCG1760
0177      18  IHLF=11                                       DHCG1770
0178          X=X+H                                         DHCG1780
0179          GOTO 4                                       DHCG1790
0180      C                                             DHCG1800
0181      C      THERE IS SATISFACTORY ACCURACY AFTER LESS THAN 11 BISECTION. DHCG1810
0182      19  X=X+H                                         DHCG1820
0183          CALL FCT(X,Y,DERY)                            DHCG1830
0184          DO 20 I=1,NDIM                               DHCG1840
0185          AUX(3,I)=Y(I)                                DHCG1850
0186      20  AUX(10,I)=DERY(I)                            DHCG1860
0187          N=3                                           DHCG1870
0188          ISW=4                                         DHCG1880
0189          GOTO 100                                     DHCG1890
0190      C                                             DHCG1900
0191      21  N=1                                           DHCG1910
0192          X=X+H                                         DHCG1920
0193          CALL FCT(X,Y,DERY)                            DHCG1930
0194          X=PRMT(1)                                     DHCG1940
0195          DO 22 I=1,NDIM                               DHCG1950
0196          AUX(11,I)=DERY(I)                            DHCG1960
0197      22  OY(I)=AUX(1,I)+H*(.375D0*AUX(8,I)+.7916666666666667D0*AUX(9,I)
0198          1-.2083333333333333D0*AUX(10,I)+.04166666666666667D0*DERY(I)) DHCG1970
0199      23  X=X+H                                         DHCG1980
0200          N=N+1                                         DHCG1990
0201          CALL FCT(X,Y,DERY)                            DHCG2000
0202          CALL OUTP(X,Y,DERY,IHLF,NDIM,PRMT)           DHCG2010
0203          IF(PRMT(5))16,24,6                            DHCG2020
0204      24  IF(N-4)25,200,200                             DHCG2030
0205      25  DO 26 I=1,NDIM                               DHCG2040
0206          AUX(N,I)=Y(I)                                DHCG2050
0207      26  AUX(N+7,I)=DERY(I)                            DHCG2060
0208          IF(N-3)27,29,200                             DHCG2070
0209      C                                             DHCG2080
0210      27  DO 28 I=1,NDIM                               DHCG2090
0211          DELT=AUX(9,I)+AUX(9,I)                        DHCG2100
0212          DELT=DELT+DELT                                DHCG2110
0213      28  Y(I)=AUX(1,I)+.3333333333333333D0*H*(AUX(8,I)+DELT+AUX(10,I)) DHCG2120
0214          GOTO 23                                       DHCG2130
0215      C                                             DHCG2140
0216      29  DO 30 I=1,NDIM                               DHCG2150

```


80/80 LIST

```

0000000001111111112222222223333333334444444455555555666666667777777778
1234567890123456789012345678901234567890123456789012345678901234567890

CARD
0001 SUBROUTINE DERFUN(TX,Y,DERY) DFUN0010
0002 C***** DFUN0020
0003 C*** ROUTINE TO EVALUATE THE ***DFUN0030
0004 C*** DERIVATIVE OF (NE) ***DFUN0040
0005 C*** TEMPERATURE COEFFICIENTS ***DFUN0050
0006 C***** DFUN0060
0007 DOUBLE PRECISION ETA1(10),ETA2(10),H,DLDT,G,TV,T,ONE,ZERO,CH2O, DFUN0070
0008 * TEND,TMIN,TPRT,PI,EL,DELI DFUN0080
0009 COMMON/COM1/ETA1,ETA2,H,DLDT,G,TV,T,ONE,ZERO,CH2O,TEND,TMIN,TPRT, DFUN0090
0010 * PI,EL,DELI, DFUN0100
0011 * N,MCOUNT,NCOUNT,NPRNT,NSTEP,ISTEP,ISTART, DFUN0110
0012 * NM1,NP1,NP2 DFUN0120
0013 DOUBLE PRECISION TX,Y(36),DERY(36),A(24), DFUN0130
0014 C DFUN0140
0015 C THE ABOVE SPECIFICATION CARDS ARE COMMON DFUN0150
0016 C TO - 'MAIN' , 'DEROUT' , & 'DERFUN' DFUN0160
0017 C THE FOLLOWING SPECIFICATIONS ARE PARTICULAR DFUN0170
0018 C TO 'DERFUN' DFUN0180
0019 C DFUN0190
0020 * DA(24),DEXP, ASUM,BSUM,CSUM,DSUM,ABSUM, DFUN0200
0021 * CDSUM,COSJPI,COSJPL,SINJPL,DCOS,DSIN DFUN0210
0022 6000 FORMAT(' ',6(E12.6)) DFUN0220
0023 9708 FORMAT('O DERFUN LEVEL 100') DFUN0230
0024 DATA NDFUN/O/ DFUN0240
0025 IF(NDFUN.EQ.O) WRITE(6,9708) DFUN0250
0026 NDFUN = 1 DFUN0260
0027 NE = N + 2 DFUN0270
0028 C***** DFUN0280
0029 C*** ***DFUN0285
0030 C***** DFUN0290
0031 10 DO 11 J=1,NP1 DFUN0300
0032 A(J) = Y(J) DFUN0310
0033 11 CONTINUE DFUN0320
0034 EL = Y(NP2) DFUN0330
0035 C***** DFUN0340
0036 C*** CALCULATION OF TEMPERATURE DERIVATIVE ***DFUN0350
0037 C***** DFUN0360
0038 20 ASUM = ZERO DFUN0370
0039 BSUM = ZERO DFUN0380
0040 CSUM = ZERO DFUN0390
0041 DSUM = ZERO DFUN0400
0042 DO 21 J=1,N DFUN0410
0043 COSJPI = DCOS(J*PI) DFUN0420
0044 COSJPL = DCOS(J*PI*EL) DFUN0430
0045 SINJPL = DSIN(J*PI*EL) DFUN0440
0046 ASUM = ASUM + (COSJPI*COSJPL) DFUN0450
0047 BSUM = BSUM + (A(J+1)*((PI*J)**2)*COSJPL) DFUN0460
0048 CSUM = CSUM + (COSJPL**2) DFUN0470
0049 DSUM = DSUM + (A(J+1)*(PI*J)*SINJPL) DFUN0480
0050 21 CONTINUE DFUN0490
0051 ASUM = (G*((2.000*ASUM)+ONE))- BSUM DFUN0500
0052 CDSUM = (H*((2.000*CSUM)+ONE))- DSUM DFUN0510
0053 DLDT = -(ABSUM/CDSUM) DFUN0520
0054 DA(1) = (H*DLDT)+G DFUN0530

```

80/80 LIST

00000000111111112222222233333333444444445555555566666666777777778
 1234567890123456789012345678901234567890123456789012345678901234567890

CARD			
0055		DO 22 J=1,N	DFUN0540
0056		ASUM = DCOS(J*PI*EL)*H*DLD	DFUN0550
0057		BSUM = ((-ONE)**J)*G	DFUN0560
0058		DA(J+1) = (2.000*(ASUM+BSUM))-(((PI*J)**2)*A(J+1))	DFUN0570
0059	22	CONTINUE	DFUN0580
0060	30	DO 31 J=1,NP1	DFUN0590
0061		DERY(J) = DA(J)	DFUN0600
0062	31	CONTINUE	DFUN0610
0063		DERY(NP2) = DLD	DFUN0620
0064		RETURN	DFUN0630
0065		END	DFUN0640

80/80 LIST

```

0000000001111111112222222223333333334444444445555555556666666667777777778
12345678901234567890123456789012345678901234567890123456789012345678901234567890
CARD
0055      DO 3 I=1,NP1                                DOUT0550
0056      II = I-1                                    DOUT0560
0057      COSPNX = DCOS(PI*II*X(10))                  DOUT0570
0058      ASUM = ASUM + (Y(II)*COSPNX)                 DOUT0580
0059      3 CONTINUE                                    DOUT0590
0060      TEMP(10) = ASUM                               DOUT0600
0061      IF(TEMP(10).LT.TV) GO TO 4                    DOUT0610
0062      IF(TEMP(10).EQ.TV) GO TO 6                    DOUT0620
0063      IF(TEMP(10).GT.TV.AND.DABS(TV-TEMP(10)).LE.O.10D-05) GO TO 6 DOUT0630
0064      T = T - DELI                                   DOUT0640
0065      DELI = DELI/0.10D+02                           DOUT0650
0066      RETURN                                         DOUT0660
0067 C*****DOUT0670
0068      6 PRMT(5) = 1.000                               DOUT0680
0069      GO TO 5                                         DOUT0690
0070      4 IF(NCOUNT.GE.NPRNT.OR.DELT.GE.TMIN) GO TO 5 DOUT0700
0071      RETURN                                         DOUT0710
0072      5 TPRT = T                                     DOUT0720
0073      NCOUNT = 0                                    DOUT0730
0074      IF(EL.GE.O.99D0) NCOUNT = 11                 DOUT0740
0075      10 DO 11 J=1,NP1                               DOUT0750
0076      A(J) = Y(J)                                   DOUT0760
0077      11 CONTINUE                                    DOUT0770
0078      EL = Y(NP2)                                    DOUT0780
0079      OLDT = DERY(NP2)                               DOUT0790
0080 C*****DOUT0800
0081 C***** CALCULATION OF *****DOUT0810
0082 C***** TEMPERATURE (X) *****DOUT0820
0083 C*****DOUT0830
0084      20 DO 21 J=1,10                                DOUT0840
0085      ASUM = ZERO                                    DOUT0850
0086      X(J) = J/10.0                                  DOUT0860
0087      DO 22 I=1,NP1                                  DOUT0870
0088      II = I-1                                       DOUT0880
0089      COSPNX = DCOS(PI*II*X(J))                      DOUT0890
0090      ASUM = ASUM + (A(II)*COSPNX)                   DOUT0900
0091      22 CONTINUE                                    DOUT0910
0092      TEMP(J) = ASUM                                  DOUT0920
0093      21 CONTINUE                                    DOUT0930
0094      30 DO 31 J=1,8                                  DOUT0940
0095      ASUM = ZERO                                    DOUT0950
0096      XX(J) = ETA1(J)*EL                             DOUT0960
0097      IF(J.GT.4) XX(J) = (ETA2(J-4)*(ONE-EL)) + EL  DOUT0970
0098      DO 32 I=1,NP1                                  DOUT0980
0099      II = I-1                                       DOUT0990
0100      COSPNX = DCOS(PI*II*XX(J))                     DOUT1000
0101      ASUM = ASUM + (A(II)*COSPNX)                   DOUT1010
0102      32 CONTINUE                                    DOUT1020
0103      TTEMP(J) = ASUM                                 DOUT1030
0104      31 CONTINUE                                    DOUT1040
0105      XX(9) = ZERO                                    DOUT1050
0106      XX(10) = ZERO                                  DOUT1060
0107      IF(MCOUNT.EQ.O) GO TO 33                      DOUT1070
0108      WRITE(7,6666) T,OLDT,EL,(I,A(I),I=1,NP1)      DOUT1080

```

80/80 LIST

```

000000001111111112222222223333333334444444445555555556666666667777777778
12345678901234567890123456789012345678901234567890123456789012345678901234567890
CARD
0109 33 WRITE(6,2999) INTSP DOUT1090
0110 WRITE(6,3000) T,DLDT,EL DOUT1100
0111 WRITE(6,5002) DOUT1110
0112 WRITE(6,2010) DOUT1120
0113 WRITE(6,2020) (I,I,A(I),I=1,NP1) DOUT1130
0114 WRITE(6,2777) DOUT1140
0115 WRITE(6,5002) DOUT1150
0116 WRITE(6,1010) DOUT1160
0117 WRITE(6,1020) (I,X(I),I=1,10) DOUT1170
0118 WRITE(6,2888) DOUT1180
0119 WRITE(6,1111) (TEMP(I),I=1,10) DOUT1190
0120 WRITE(6,5002) DOUT1200
0121 WRITE(6,1020) (I,XX(I),I=1,8) DOUT1210
0122 WRITE(6,2777) DOUT1220
0123 WRITE(6,2888) DOUT1230
0124 WRITE(6,1111) (TTEMP(I),I=1,8) DOUT1240
0125 WRITE(6,2777) DOUT1250
0126 WRITE(6,5002) DOUT1260
0127 IF(NSTEP.EQ.0) GO TO 34 DOUT1270
0128 ISTEP = ISTEP + 1 DOUT1280
0129 IF(ISTEP.GE.NSTEP) GO TO 40 DOUT1290
0130 34 IF(T.GE.TEND) GO TO 40 DOUT1300
0131 IF(EL.LE.0.100-01) GO TO 50 DOUT1310
0132 RETURN DOUT1320
0133 40 WRITE(6,5000) NSTEP DCUT1330
0134 STOP DOUT1340
0135 50 WRITE(6,6000) DOUT1350
0136 STOP DOUT1360
0137 END DOUT1370

```

VITA

Lawrence Barry Samartin

Candidate for the Degree of

Master of Science

Thesis: VAPORIZATION INTERFACE PROPAGATION THROUGH A ONE-DIMENSIONAL
POROUS SLAB

Major Field: Mechanical Engineering

Biographical:

Personal Data: Born in Newark, New Jersey, July 28, 1941, the son
of Mr. and Mrs. Louis J. Samartin.

Education: Graduated from Union High, Union, New Jersey, in June,
1959; received Bachelor of Arts in Secondary Mathematics
Education degree from Newark State College in 1963; attended
Stevens Institute of Technology, 1965-66; completed the
requirements for the Master of Science degree at Oklahoma
State University in May, 1973.

Professional Experience: Secondary Mathematics Teacher, Union
County Regional High School District No. 1, Berkley Heights,
New Jersey, 1963-64; Computer Programmer, Western Electric
Company, 1965-66; Communication Computer Systems Analyst,
United States Air Force, 1967-69; Research Assistant,
School of Mechanical and Aerospace Engineering, Oklahoma
State University, 1970-72.